

1 **Introducing standardized field methods for fracture-focused surface**
2 **processes research**

3 Martha Cary Eppes¹, Jennifer Aldred², Samantha Berberich¹, Maxwell P. Dahlquist³, Sarah G. Evans⁴,
4 Russell Keanini⁵, Faye Moser¹, Mehdi Morovati⁵, Steven Porson¹, Monica Rasmussen¹, Alex Rinehart⁶, Uri
5 Shaanan⁷

6 ¹ Department of Geography & Earth Sciences, University of North Carolina at Charlotte, Charlotte, NC 28223, USA

7 ² New Mexico Highlands University, Las Vegas, NM, USA

8 ³ Department of Geology, University of the South, Sewanee, TN 37383, USA

9 ⁴ Department of Geological and Environmental Sciences, Appalachian State University, Boone, NC, 28608, USA

10 ⁵ Department of Mechanical Engineering and Engineering Science, University of North Carolina at Charlotte, Charlotte, NC
11 28223, USA

12 ⁶ Department of Earth and Environmental Sciences, New Mexico Institute of Mining and Technology, Socorro, NM, 87801,
13 USA

14 ⁷ Geological Survey of Israel, Jerusalem 9692100, Israel

15 *Correspondence to:* meppes@uncc.edu

16

17 **Abstract.** Rock fractures comprise a key contributor to a broad array of Earth surface processes due to their direct control on rock
18 strength as well as rock porosity and permeability. However, to date, there has been no standardization for the quantification of
19 rock fractures in surface processes research. In this work, the case is made for standardization within fracture-focused research and
20 prior work is reviewed to identify various key datasets and methodologies. Then, a suite of standardized methods is presented as a
21 ‘baseline’ for fracture-based research in surface processes studies. These methods have been shown in preexisting work from
22 structural geology, fracture mechanics, and surface processes disciplines to comprise best practices for the characterization for
23 fractures in clasts and outcrops. These practical, accessible, and detailed methods can be readily employed across all fracture-
24 focused weathering and geomorphology applications. The wide adoption of a baseline of data collected using the same methods
25 will enable comparison and compilation of datasets among studies globally and will ultimately lead to a better understanding of
26 the links and feedbacks between rock fracture and landscape evolution.

27

28 **Short Summary.** All rocks have cracks that can influence virtually every process acting on Earth's surface where humans live.
29 Yet, scientists have not standardized their methods for collecting crack data. Here we draw on past work across geo-disciplines to
30 show why standardization is important and propose a list of baseline data for fracture-focused surface processes research. We detail
31 its rationale and the methods for collecting it. We hope its wide adoption will improve knowledge of rock fracture overall.

32 1 Introduction

33 Rock fracture in surface and near-surface environments plays a key role in virtually all Earth surface processes. The propagation
34 of opening-mode fractures in universality occurs at or near the surface of Earth (e.g., within ~500 m - Moon et al., 2020), on other
35 terrestrial bodies (Molaro et al., 2020), and at depth in the crust (e.g., Laubach et al., 2019). It epitomizes mechanical weathering
36 and the development of ‘critical zone architecture’, i.e., the evolving porosity, permeability, and strength of near-surface rock (e.g.,
37 Riebe et al., 2021). For clarity and consistency herein, the use of the term fracture is limited to refer to any *open*, high-aspect ratio
38 discontinuity in rock, regardless of its location (within a clast, or within shallow or deep bedrock), origin, or scale, acknowledging
39 that veins or dikes (filled with secondary minerals) are also termed ‘fractures’ in many contexts. The term ‘crack’ is avoided
40 because the wide-ranging semantics of the term can cause confusion when employed in interdisciplinary work across rock
41 mechanics, structural geology, and geomorphology.

42

43 Fracture characteristics (e.g. size, number, connectivity, orientation) exert enormous influence on both rock mechanical properties
44 (e.g., Ayatollahi and Akbardoost, 2014) and rock hydrological properties (e.g., Leone et al., 2020; Snowden et al., 2021). Fractures
45 therefore influence a wide array of natural and anthropogenic landscape features and processes including channel incision (e.g.,
46 Shobe et al., 2017), sediment size and production (Sousa, 2010; Sklar et al., 2017), hillslope erosion (e.g., DiBiase et al., 2018;
47 Neely et al., 2019), built environment degradation (e.g., Hatir, 2020), landslide and rockfall hazards (e.g., Collins and Stock, 2016),
48 groundwater and surface water processes (e.g., Maffucci et al., 2015; Wohl, 2008), and vegetation distribution (e.g., Aich and
49 Gross, 2008). Additionally, the resultant physical properties of fracturing-produced sediment (i.e., clast size distribution, mass,
50 porosity, etc.) control both hillslope and stream processes (e.g., Chilton and Spotila, 2020; Glade et al., 2019).

51

52 With fractures clearly central to so many surface processes, as well as non-academic concerns of hazard and infrastructure
53 degradation, it is crucial to understand the factors that control surface and near-surface rock fracture attributes and rock fracturing

54 rates and processes. To fully do so requires a large body of data quantifying fracture-related characteristics and phenomena in a
55 variety of subaerial environments; however, to date, no standard field methods have been widely adopted to quantify fractures in
56 the modern surface processes realm. Consequently, data collected across studies cannot be readily compared or coalesced. The
57 purpose of this paper is to define an initial set of such standards by combining prior fracture methodology studies from other
58 geoscience disciplines with those that have been developed, tested and refined during more than 20 years of field-based fracture
59 observations for surface processes-related research (e.g., Aldred et al., 2015; Eppes and Griffing, 2010; Eppes et al., 2018; Eppes
60 et al., 2010; Mcfadden et al., 2005; Moser, 2017; Shobe et al., 2017; Weiserbs, 2017).

61
62 Building on this combination of past work, this paper first defines the benefits of establishing a standard procedure for fracture-
63 focused surface processes field research, describing how the authors' chosen methods outperform other approaches. This is limited
64 to in-person field observations on sub-aerially exposed rock - i.e., fractures that can be observed with the naked eye or basic hand
65 lens. Measurements of smaller fractures (e.g., those visible with microscopy) or of buried fractures (e.g., those visualized in
66 boreholes or with indirect geophysical methods) are not directly described here. Also, methods for fracture detection using rapidly
67 evolving automated analyses of remote data such as LiDAR, drone photography, or structure-from-motion are not described. These
68 technologies hold great promise for expanding the scope of fracture measurements, but to date also hold numerous limitations. The
69 methods outlined herein could be employed for the consistent validation of such data in the future.

70
71 The overall aim of this paper is to build: 1) a set of guiding principles applicable to all surface processes research involving rock
72 fractures; 2) a list of fracture and rock data measurements that constitute "basic" field-based metrics; and 3) practical methods that
73 comprise best practices for collection of these data. Unless otherwise specified, all methods may be applied to loose clasts or to
74 outcrops. Also provided are some suggestions for data analyses and a demonstration of a real case example of how the proposed
75 methods lead to reproducible results across users. By providing this compendium of fracture-focused field methods, the hope is to
76 accelerate understanding of how a most basic feature of all rock – its open fractures – contributes to the processes and evolution
77 of Earth's surface and critical zone.

78 **1.1 The value of a standardized approach**

79 Particularly within the fields of geomorphology and weathering sciences, no common suite of data, methods, or terminology has
80 been defined or described that comprises an analysis of fractures. Although fracture characterization field methods exist in the
81 context of structural geology and aquifer and reservoir characterization (e.g., Watkins et al., 2015; Wu and Pollard, 1995; Zeeb et
82 al., 2013; Laubach et al., 2018), they diverge significantly in their approaches because they were largely developed for the specific
83 application of each unique study or field of study. Furthermore, the terminology and methodology used to describe natural fractures
84 across this existing research are largely limited to only those fractures loosely interpreted to be tectonically induced 'joints', and
85 numerous published works fail to provide clear criteria, even for choosing which fractures to measure. This lack of consistency
86 severely limits the ability of the geomorphic community to reproduce methods, or to combine, compare, or interpret different
87 fracture datasets.

88
89 The development of consistent methods undergirds most quantitative Earth sciences. For example, the fields of sedimentology and
90 soil science have clear, standardized methods to acquire what constitutes the "basic" data for their observations. Sedimentologists

91 have long shared common metrics and methods for quantifying grain size, sorting, rounding, and stratigraphic records (e.g.,
92 Krumbein, 1943). Similarly, soil scientists share common methods, metrics, and nomenclature for describing soil profiles and
93 horizons (e.g., Birkeland, 1999 Appendix A; Soil Survey Staff, 1999). The realization of the need for standard methods has also
94 remained constant in laboratory-based rock mechanics over the last several decades, driving the American Society for Testing and
95 Materials (ASTM) and International Society for Rock Mechanics (ISMR) to publish ongoing standards and methods papers (e.g.,
96 Ulusay and Hudson, 2007; Ulusay, 2015).

97
98 Standards like those mentioned above exist because workers have long recognized and reaped their benefits. Standardized methods
99 can frequently lead to major step-change innovations when data are combined. For example, standardized soil methods allowed
100 for 100 m scale mapping across the United States, enabling detailed human–landscape models that can aid in preserving vital soil
101 resources (Ramcharan et al., 2018). In the field of rock mechanics prior to the 1950s, theoretical developments of rock failure and
102 plasticity lagged behind other branches of geophysics and engineering, limited both by technology and, arguably more so, by lack
103 of consistent methods. Methods for repeatable failure testing were then developed, largely in the groups led by Knoppf, Griggs,
104 and Turner in the United States and Australia (Wenk, 1979). This standardization culminated in the landmark series of papers that
105 comprised the observations driving 50 subsequent years of experimental rock mechanics (e.g., Borg and Handin, 1966; Handin et
106 al., 1963; Handin and Hager, 1957, 1958; Heard, 1963; Mogi, 1967, 1971; Turner et al., 1954).

107
108 Here, a set of methods is proposed as a starting point for surface processes researchers so that a larger community of teams can
109 begin to cross-pollinate their observations. It is necessary and expected that these methods will evolve as new needs and
110 applications arise.

111 112 **1.2 Development of the standardized fracture measurement approach**

113 For the specific case of fracture-focused research, outside of geomorphology applications, the need for standardized rule-based
114 methods has already been established. Within this prior body of research and, when considered in the context of surface processes
115 problems, the methods proposed below have been shown to outperform other approaches. In one case example, study participants
116 were asked to measure fractures with no particular instructions given for how to collect the data other than where to collect it. The
117 wide variance in resulting datasets collected by different users led to the conclusion that, without common and clearly established
118 measurement and selection criteria, fracture characterization is rife with subjective bias that severely impacts interpretations of
119 results (Andrews et al., 2019). Then, based on post-data collection interviews and workshops, Andrews et al. (2019) scrutinized
120 the source of the variance and provided a list of suggested best-practices that would serve to best eliminate the subjectivity of data
121 collection that was leading to the bias. Forstner and Laubach (2022) and Ortega and Marrett (2000) further detail that many such
122 issues arise, particularly from a lack of specificity with respect to identifying features to be measured.

123
124 In another case example, Zeeb et al. (2013) sought to determine how different sampling approaches lead to censoring bias of
125 different fracture sizes from outcrop data by applying different sampling methods to artificially generated fracture networks that
126 had known parameters. Analysis of data collected using scanline, window, and circular estimator methods revealed that the window
127 approach resulted in the lowest uncertainty for most parameters and required the fewest measurements to provide representative
128 datasets.

129

130 Incorporated here are the suggested best practices from the two case examples above as well as from other published methods
 131 research. Some methods are well attested to be reproducible in field studies. For example, field measurement ‘crack comparators’
 132 are effective for measuring opening displacements particularly for sub-millimeter widths (e.g., Ortega et al., 2006). Other
 133 measurements such as length and connectivity may have low reproducibility (Andrews et al., 2019) owing to various observational
 134 and conceptual problems, including dependence on scale of observation (e.g., Ortega and Marrett, 2000). Above all, it is clear that
 135 reproducibility requires clear, rule-based criteria for all decision-making (Forstner and Laubach, 2022).

136

137 The chosen standardized methods are optimized for collecting outcrop- and clast-fracture data relevant to geomorphology. The
 138 methods described herein are germane to surface and near-surface (< 0.5 km) studies such as validating geophysical measurements,
 139 testing factors that influence fracture formation, or documenting links between fracture characteristics and topography or sediment
 140 production. These methods possibly differ from those of studies with other goals, such as using outcrops as guides (analogs) for
 141 deep (km scale) subsurface fractures. Such studies aim to distinguish mechanical and fracture stratigraphy, corroborate fracture
 142 patterns related to features (i.e., folds), obtain fracture statistics for discrete fracture models, or test efficacy of forward
 143 geomechanical fracture models. For these studies examining deeper deformation, mineral filled fractures may be more useful or
 144 appropriate than open fractures. Also, for these applications, near-surface and geomorphology-related fractures are considered
 145 “noise” and need to be omitted (e.g., Sanderson, 2016; Ukar et al., 2019). However, a major outstanding question is how this might
 146 be reasonably and accurately accomplished given the relatively sparse number of studies of fractures in the context of
 147 geomorphology.

148 **2 Standardized methods: Guiding principles**

149 **2.1 Natural rock fracturing background**

150 The design of any fracture-related study in the context of surface processes must arise from consideration of the variables that may
 151 influence the rates of fracturing and the characteristics of the fractures that form. When rock is proximal to Earth’s surface, those
 152 variables include factors related to Earth’s topography, atmosphere, biosphere, cryosphere, and/or hydrosphere. Here, a very brief
 153 overview is provided of some key rock fracture mechanics concepts behind these factors. Eppes and Keanini (2017) and Eppes
 154 (2022) provide more detailed reviews of rock fracture processes in the context of surface processes.

155

156 Rocks fracture at and near Earth’s surface in response to the complex sum of all tectonic (e.g., Martel, 2006), topographic (e.g.,
 157 St. Clair et al., 2015; Moon et al., 2020; Molnar, 2004), biological (e.g., Brantley et al., 2017; Hasenmueller et al., 2017), and
 158 environment-related (e.g., Matsuoka and Murton, 2008; Gischig et al., 2011) stresses they experience. Fracturing can occur when
 159 stresses exceed the failure criteria (i.e., short-term material strength). More commonly, however, because critical stresses are only
 160 rarely reached in nature, fractures can also propagate *subcritically* at stresses as low or lower than 10% of the rock’s strength (see
 161 textbooks such as Schultz, 2019; Atkinson, 1987).

162

163 Overall, subcritical fracture propagation rates and processes are strongly dependent on stress magnitude, but they are *also* strongly
 164 influenced by the size of the fracture that is under stress, as well as the environmental conditions that impact fracture tip bond
 165 breaking (see fracture mechanics textbooks such as Anderson, 2005; or reviews such as Laubach et al., 2019). For single isolated

166 fractures, stresses applied to the rock body are concentrated at fracture tips proportional to the length of the fracture (a concept
 167 embodied by the term ‘stress intensity’), effectively increasing the stresses experienced directly in that location. The environmental
 168 factors known to impact subcritical rock cracking - in a manner separate from their influence on stresses - include vapor pressure,
 169 temperature, and pore-water chemistry (Eppes and Keanini, 2017; Eppes et al., 2020; Brantut et al., 2013; Laubach et al., 2019).
 170 Therefore, in the context of surface processes, climate matters twice for rock fracturing: 1) as it contributes to the stresses that the
 171 rock experiences, and 2) as it contributes to the chemo-physical processes that break bonds at fracture tips as they propagate
 172 subcritically.

173
 174 Just as other common physical properties like tensile strength can be measured, rocks can be tested for their propensity to fracture
 175 subcritically by the measurement of subcritical cracking parameters such as the subcritical cracking index (e.g., Paris and Erdogan,
 176 1963; Chen et al., 2017; Holder et al., 2001; Nara et al., 2012; Nara et al., 2017). These parameters influence both the rate of
 177 subcritical cracking in rock and the fracture characteristics (e.g., amount of fracture per area or fracture length as in Olson, 2004).
 178 In sum, natural rock fracturing is not necessarily the singular, catastrophic event as it frequently portrayed in surface processes
 179 research. Instead, it is likely dominantly a slowly evolving process progressing over geologic time and influenced by complex
 180 feedbacks between rock and fracture properties, as well as environmental, topographic, and tectonic factors.

181 2.2 Site selection and study design using a “State Factor” approach

182 Due to their influence on rock fracturing as described above, all potential driving stresses and variations in fracture environments
 183 must be considered in site selection and study design for any fracture-related research. Parent material, topography (and other
 184 loads), climate, biota, and time all potentially impact initiation and propagation of surficial fractures in rocks. Though this idea
 185 might generally exist in other fracture-focused research, in the field of soil geomorphology it has long been explicitly described as
 186 a ‘State Factor’ approach (e.g., Jenny, 1941; Phillips, 1989) to understanding progressive chemical and physical alteration
 187 processes. Thus, we propose that this well-vetted conceptual paradigm may be employed as a standard.

188
 189 Here, it is asserted that applying a State Factor approach to fracture research is relevant because fracturing processes are influenced
 190 by each of these factors, just as all other chemical processes acting on rock and soil. This is particularly true when the subcritical
 191 nature of rock fracture is considered (Sect. 2.1). Thus, all State Factors that could contribute to fracture propagation styles, and
 192 rates should be explicitly considered and controlled for as much as possible within the aims and scope of the research for any given
 193 site. These ‘State Factors’ - long categorized as they relate to overall soil development, of which physical weathering is a
 194 component (e.g., Jenny, 1941) - are equally applicable to fractures alone, and include climate (cl, both regional climate and
 195 microclimate), organisms (o, flora and fauna), relief (r, topography at all scales), parent material (p, rock properties) and time (t,
 196 exposure age or exhumation rate). For rock fracture, tectonics (T) should be added to this list, making cl,o,r,p,t,T.

197
 198 Hereafter, the term ‘site’ refers to a single location of either a group of rock clasts or a group of outcrops, whereby all clasts or
 199 outcrops within the ‘site’ could be reasonably assumed to have experienced similar State Factors over their exposure history. For
 200 example, a site might comprise a single boulder bar on an alluvial fan surface or a single ridgeline with several outcrops. Once the
 201 specific State Factors (including the internal variability of each site) are identified for all the sites within a given field area, a series

202 of sites can be selected whose State Factors are known and controlled for as much as possible. This enables a study of the influence
 203 of individual factors across the sites, i.e., fracture chronosequences, climosequences, toposequences, or lithosequences.

204

205 For rock fracture, it is important to understand how each cl,o,r,p,t,T factor may contribute both to stresses that give rise to fracturing,
 206 and/or to the molecular-scale processes that serve to subcritically break bonds at fracture tips (Sect. 2.1). Each has the potential to
 207 independently impact fracturing rates, styles, and processes. The following descriptions provide only brief examples of how each
 208 of the State Factors may influence rock fracture. To fully describe each of their influences on rock fracturing would comprise a
 209 textbook. The factors are listed in the cl,or,r,p,t,T order by traditional convention only. Assuredly, to date, there are insufficient
 210 data to propose a hierarchy of their influence on fracture characteristics in surface processes contexts.

211 2.2.1 Climate (cl)

212 *Climate (cl)* as a State Factor refers not just to regional mean annual precipitation or temperature, but also the local microclimate
 213 of a site, which may be influenced by site characteristics, such as runoff or aspect. The presence of liquid water increases the
 214 efficacy of water-related stress-loading processes like those related to freezing (Girard et al., 2013) or chemical precipitation of
 215 salts or oxides (e.g., Buss et al., 2008; Ponti et al., 2021). Moisture – particularly vapor pressure – can also serve to accelerate rock
 216 fracturing rates independent of any stress-loading (e.g., Eppes et al., 2020; Nara et al., 2017). Temperature cycling can produce
 217 thermal stresses (through differential expansion and contraction of both adjacent minerals as well as different portions of the rock
 218 mass, e.g., Ravaji et al., 2019), and can also influence rates and processes of fracture-tip bond breaking (e.g., Dove, 1995).

219 2.2.2 Organisms (o)

220 *Organisms (o)* refers to both flora and fauna - everything from overlying vegetation and large animals to roots and microorganisms,
 221 all of which may provide a source of rock stress and/or may influence water availability or chemistry. These relationships can be
 222 complex and unexpected. For example, tree motion during wind and root swelling during water uptake both exert stresses on rock
 223 directly (Marshall et al., 2021a). Organism density and type can impact rock water and air chemistry (Burghelca et al., 2015), both
 224 of which may impact the rates and processes of subcritical cracking (e.g., review in Brantut et al., 2013).

225 2.2.3 Relief (r)

226 In the context of State Factors, *relief (r)* refers generically to all metrics related to topography including aspect, slope, and
 227 convexity. Topography impacts the manifestation of both gravitational stresses, as well as tectonic stresses within the rock body
 228 (Molnar, 2004; Moon et al., 2020; Martel, 2006). The directional aspect of a particular outcrop or boulder face may also influence
 229 insolation and water retention, translating into differences in microclimate and vegetation and, thus, weathering overall (e.g.,
 230 Burnett et al., 2008; West et al., 2014; Mcauliffe et al., 2022), including fracturing (e.g., West et al., 2014).

231 2.2.4 Parent material (p)

232 The *parent material (p)* factor in the context of a fracture study refers to the specific rock type(s) containing fractures (and
 233 potentially undergoing fracture) in the geomorphic environment. Rock varies in the types and dimensions of material present (e.g.,
 234 sandstone, siltstone, shale, basalt, granite etc.) and the types and spatial arrangements of interfaces within the material (e.g., grain
 235 size, porosity, bedding, foliation). These properties directly influence the rates and styles of fracture propagation (Atkinson, 1987)

236 due to both how they respond to stresses but also due to how they allow stresses to arise. Thus, they can all influence the rates and
 237 characteristics of fracture growth and susceptibility to topographic and environmental stresses. For example, different minerals are
 238 characterized by different coefficients of thermal expansion. As a result, rocks with different mineral constituents will be more or
 239 less sensitive to thermal stresses than others depending on the contrasts between adjacent grains. Rock mineralogy will also impact
 240 chemical processes acting at crack tips during subcritical cracking, as well as the overall susceptibility of the rock to chemical
 241 weathering.

242
 243 Many (perhaps most) rocks contain fractures that formed prior to exposure, either due to deep seated tectonics and fluid pressure
 244 loads or to thermal and mechanical effect due to uplift towards the surface (English and Laubach, 2017; Engelder, 1993). In
 245 sedimentary rocks, fracture patterns (and, in some cases, fracture stratigraphy) vary with mechanical stratigraphy (e.g., Laubach et
 246 al., 2009) that can also influence near-surface fracture. In many instances, mechanical properties may be reflected in fracture
 247 stratigraphy, and vice versa. Schmidt hammer measurements are a useful, fast, and inexpensive field approach to documenting
 248 mechanical property variability (Aydin and Basu, 2005), however such measurements are impacted by weathering exposure age
 249 (Matthews and Winkler, 2022). The influence of fracture characteristics of the parent rock that may have formed in the deep
 250 subsurface are described in Sect. 2.2.6 “Tectonics”.

251
 252 Additionally, here, parent material also refers to the size and shape of the clast or outcrop. For example, angular corners generally
 253 concentrate stresses more than rounded edges (Anderson, 2005). Also, clasts or outcrops of different sizes experience different
 254 magnitudes of thermal stresses related to diurnal heating and cooling (Molaro et al., 2017).

255 2.2.5 Time (t)

256 *Time (t)* likely plays a role in rock fracturing rates just as it does in chemical weathering, whereby outcrops found in slowly-eroding
 257 environments or clasts on old surfaces may be subject to different fracturing rates and processes (e.g., Rasmussen et al., in prep;
 258 Mushkin et al., 2014). Over time, rock mechanical properties can also change as weathering occurs (e.g., Cuccuru et al., 2012).
 259 Although the time factor has not been well-studied in the context of natural rock fracture, preliminary data suggest that it should
 260 be considered (Berberich, 2020; Rasmussen et al., 2021). Published surficial geologic maps or datasets of rock exposure ages or
 261 erosion rates (e.g., Balco, 2020) will provide such ‘time’ information.

262 2.2.6 Tectonics (T)

263 Finally, in a fracture-related study, *tectonic (T)* setting must also be considered as a State Factor. Fractures that have formed in the
 264 deep subsurface in response to tectonic forces inevitably become exhumed. Overall, tectonic fractures have traditionally been
 265 studied within the structural geology discipline, and that literature is extensive (e.g., reviews in Laubach et al., 2019; Laubach et
 266 al., 2018; Atkinson, 1987, Chapter 2). The tectonic history of rock can be maintained in its brittle structures over a wide range of
 267 past tectonic events, including its most recent exhumation and cooling. The resulting open or filled fractures depend on how deeply
 268 the material was buried, how rapidly uplifted, and the material properties (e.g., English and Laubach, 2017). Finally, the fact that
 269 the current tectonic setting can drive ongoing deformation has long been recognized (e.g., Hooke, 1972), and more recent work
 270 has highlighted that very low magnitude tectonic stresses can translate to fracture propagation in very near-surface bedrock,
 271 especially when interacting with local topography (e.g., Martel, 2011; Moon et al., 2020).

272

273 It is likely, though perhaps not widely appreciated, however, that tectonic fractures further increase in both number density (total
 274 number of fractures per area) and intensity (total fracture length per area) as they approach the surface and are propagated further
 275 by rock interactions with topographic and environmental stresses. There is a growing body of data pointing to such surface
 276 interactions (e.g., Marshall et al., 2021b; Moon et al., 2019; Moon et al., 2020; St. Clair et al., 2015), but overall, these
 277 differentiations are a topic ripe for further study. Pre-existing fractures may not always be easily separable from those formed or
 278 further propagated under geomorphological influence. Environmental stresses also produce parallel fractures (e.g., Aldred et al.,
 279 2015; Eppes et al., 2010; Mcfadden et al., 2005), as do those related to the morphology of the eroding landscape (Leith et al.,
 280 2014). For outcrops, and particularly for clasts where correlations with regional tectonic structures are not possible, microstructure
 281 analyses that examines fractures for diagenetic cements, fluid inclusions, or other similar features may provide insights into the
 282 tectonic origin of fractures.

283

284 Thus, in choosing study sites, consideration should be made of rock age, tectonic history and current tectonic setting (e.g., World
 285 Stress Map, Heidbach et al., 2018), as well as unambiguously tectonically-related structures such as dipping bedding planes,
 286 evidence of mineral deposits in the fractures, stylolites, or ductile structures such as folds (Hancock, 1985; Laubach et al., 2019).

287 **2.3 Bedrock outcrops versus deposited clasts**

288 The fracture characteristics of outcrops have long been employed as proxies for subsurface fracture networks, and there is a
 289 reasonably large body of literature addressing these relationships and their potential pitfalls (e.g., Ukar et al., 2019; Al-Fahmi et
 290 al., 2020; Sharifigaliuk et al., 2021). However, as mentioned above, topographic and environmental stresses have likely both
 291 contributed to any sub-aerially observed fracture network. Thus, for studies that aim to isolate fractures associated with
 292 environmental stresses, measurements from clasts may be more useful than outcrops.

293

294 Clasts that have been transported by fluvial, glacial, or mass-wasting processes have experienced abrasion, and therefore, it is
 295 highly likely that pre-existing superficial fractures have been removed. Thus, clasts may be more reasonably considered ‘fresh’
 296 than an outcrop with an unknown exhumation history, allowing clearer linkages between environmental exposure and observed
 297 fractures. This idea of “resetting” fractures within clasts through transport is supported by data showing clasts of identical rock
 298 type that have experienced more transport (i.e., rounded river rocks) having higher strength than those found in, for example, recent
 299 talus slopes (Olsen et al., 2020).

300 **3 Selecting the clasts, outcrops, or rock surface locations that will comprise the fracture observation area**

301 Carefully selecting the rock surface area(s) on which fractures will be observed and measured within a site is equally as important
 302 as selecting the site or the fractures themselves. Hereafter, the term ‘observation area’ refers to the specific portion(s) of rock
 303 surface(s) for which fractures are being measured. Observation areas may comprise the entire exposed surface of individual clasts,
 304 outcrops, or portions of either (Fig. 1). In the following sections, instructions for selecting these observation areas in the field are
 305 provided.

306 **3.1 Establishing outcrop or clast selection criteria**

307 Before observation areas can be identified, outcrops or clasts must be selected. The first step of that selection process is to establish
 308 criteria for determining which outcrops or surface clasts within the site are acceptable for measurement. Similar to site selection,
 309 variability in cl,o,r,p,t,T factors that may influence fracturing (temperature, moisture availability, rock shape, and rock type) should
 310 be controlled for as much as possible.

311
 312 In general, characteristics of the clasts or outcrops that might impact mechanical properties, moisture, or thermal stress-loading
 313 should be most heavily considered. The rock type properties that should be considered when developing selection criteria include
 314 not only heterogeneities like bedding or foliation, but also grain size and mineralogy, all of which can influence fracture rates and
 315 style characteristics. For example, perhaps only outcrops with no visible veins or dikes will be employed; or only outcrops greater
 316 than 1 m in height; or only north facing outcrop faces. Past work, for example, has focused on upward facing surfaces of outcrops
 317 or large clasts (e.g., Berberich, 2020; Eppes et al., 2018).

318
 319 For loose clasts, only clasts of a particular size or rock type might be employed for measurement. For example, past work found
 320 that below approximately 5 cm diameter in semi-arid and arid environments (Eppes et al., 2010), and 15 cm in more temperate
 321 environments with vegetation (Aldred et al., 2015), clasts are more likely to have been moved or disturbed. Thus, these sizes were
 322 employed as a threshold for selection.

323 **3.2 Non-biased selection of clasts or outcrops for measurement**

324 Once criteria are defined, clasts or outcrops meeting those criteria must be chosen for the fracture measurements. A procedure
 325 similar to the well-vetted Wolman Pebble Count style transect (Wolman, 1954) should be employed to avoid sampling bias. For
 326 landforms with other geometries, a grid may be used instead of a transect line.

327
 328 In either case, a tape transect or net grid is laid out on the ground at each site, and the clast or outcrop closest to specified intervals
 329 on the tape (or at the points of the grid meeting the criteria) is selected (Fig. 1a). The interval or grid spacing should be adjusted to
 330 the overall size and abundance of clasts or outcrops found on the surface. If there are relatively few meeting the criteria at a site,
 331 all within the site meeting the criteria can be measured.

332
 333 A similar technique can and should be applied for selecting outcrops. For example, care should be taken to not be limited to the
 334 ‘best’ outcrops (cleanest and/or largest), since they likely are the least fractured. For locations where outcrops are within a few
 335 meters or tens of meters of each other and vegetation relatively sparse, a grid of a set dimension (e.g., 100 m) is overlain on aerial
 336 imagery, and the closest outcrop to each grid intersection meeting the outcrop criteria are selected (Watkins et al., 2015). For areas
 337 where outcrops are not visible in aerial imagery, a measured or paced transect can be employed where the user walks along a
 338 bearing and chooses the closest outcrop meeting the selection criteria at each interval, e.g., 30 paces.

339
 340 In all of the above, transect locations and orientations should be selected following consistent criteria and being mindful of the
 341 State Factors cl,o,r,p,t,T. For example, all transects or grids might be placed uniformly along backslopes with a certain upslope
 342 distance from the crest; or along the latitudinal center or crest of a landform. Alternatively, the transect might be orientated

343 perpendicular or oblique to a paleo-flow direction so that it is not constrained only to bars or swales. The coordinates and bearing
 344 of all transects or grids should be recorded, enabling tracking and avoiding repetition.

345 **3.3 Observation areas comprising the entire clast or outcrop surface**

346 The observation area for small clasts and outcrops can be their entire exposed surface. When clasts or outcrops selected for
 347 measurements are less than ~50 cm in maximum dimension, measurements can typically be readily made for all fractures visible
 348 on the clast or outcrop exposed surface.

349
 350 No rocks should be moved during measurement. This non-disturbance practice is particularly crucial for maintaining Earth's
 351 geodiversity (Brilha et al., 2018) and preserving sites for future workers to revisit. Further, research examining acoustic emission
 352 localization of rocks naturally fracturing found that the large majority of fracture 'foci' were located in the upper hemispheres of
 353 boulders (Eppes et al., 2016). Thus, the potential insight gained by moving clasts does not warrant its damage to geoheritage.

354 **3.4 Establishing 'windows' as the observation area for larger clasts and outcrops**

355 When it is not feasible to measure every fracture on an outcrop or clast, the observation area may comprise predetermined
 356 'windows' of representative decimeter- to meter-scale areas of the rock surface (Fig. 1b). This window selection method results in
 357 an accurate representation of fractures on an entire outcrop (e.g., Zeeb et al., 2013) and is least affected by subjective bias (Andrews
 358 et al., 2019). Other techniques that require measurements of all fractures that intersect a line (scanlines) are common and effective
 359 (Marrett et al., 2018; Hooker et al., 2009), but do not provide an observation area. Consequently, they do not capture all fracture
 360 orientations, they preclude calculations of fracture number density and fracture intensity (Sect. 6.1), and they complicate
 361 determination of rock properties. For areas with large outcrop exposures, circular scanlines combined with a window approach
 362 have proven effective (Watkins et al., 2015). Scanlines are also helpful in characterizing simple fracture clustering attributes. Here,
 363 a 'window' approach is outlined that can be employed regardless of outcrop size or fracture number density. An expansion of
 364 fracture length measurements – similar to that proposed by Weiss (2008) – is also detailed so that long fractures are not
 365 underrepresented (see Sect. 5.4.1 for length methods).

366
 367 Importantly, the number and size of windows observed on each outcrop or at each site will depend on the typical number and size
 368 of fractures present on the surface of the rock (Sect. 4.2). Overall, it is preferable to strike a balance between window size and
 369 number so that during data analysis, variance can be quantified by comparing data collected between windows on the same outcrops
 370 and at the same site. More total observation area (more and/or larger windows) is required when fractures are fewer per area. The
 371 size of the area required for a representative quantification of fractures depends both on fracture average length and number density
 372 (e.g., Zhang, 2016). Here, an iterative approach is outlined for determining if sufficient area has been examined (Sect. 4.2), but
 373 other rules of thumb exist, particularly in the Rock Quality Designation Index literature (e.g., Zhang, 2016).

374
 375 Choosing the placement of windows on the outcrop should entail a stratified random sampling approach. Just as for clast- or
 376 outcrop-selection, c,l,o,r,p,t,T factors like aspect should be taken into consideration and controlled for as much as possible in the
 377 window placement strategy by, for example, only using upward facing surfaces. Then, window placement determination is made
 378 to avoid sampling bias and also edge effects. For example, if upward facing outcrop surfaces are to be characterized, then the total

379 length and width of the face could be employed to align sufficient numbers of windows along even intervals of those measurements
 380 (e.g., for example, three windows whose centers are located along the center axis of the rock with even spacing between the edges
 381 and each box; Fig. 1b).

382
 383 For the placement of each window, a simple cardboard template of the appropriate window size with a center hole can be employed
 384 to trace with chalk the window directly on the clast or outcrop. Then, all fracture measurements are made in the window(s). Each
 385 window should be numbered and photographed in the context of each outcrop or clast. Detailed photo-documentation and
 386 coordinates to 0.00000 dd are also recommended.

387 **3.5 How many observation areas?**

388 The number of clasts, outcrops, or windows required to measure sufficient fractures will vary with the study goals, site complexity,
 389 and the variables for which the data are being tested or controlled. Importantly, for each study, the required number of observation
 390 areas must be established based on the amount that is necessary to gain a statistically sufficient number of fracture observations to
 391 represent the rocks in question for that setting (Sect. 4.2). As yet, no rule-of-thumb can be employed, because there has not been
 392 sufficient standard fracture data collected to establish such a rule. Establishing such a rule of thumb is an illustration of the
 393 motivation of this paper, as well as an example of how it can be expected that the methods herein might evolve over time.

394
 395 Rocks or outcrops with lower fracture number density (fewer overall fractures per area) will require that larger areas of their surface
 396 be examined in order to measure sufficient fractures for statistical significance (Sects. 3.4 and 4.2). Rocks or outcrops with
 397 significant variation in fracture patterns require sufficient observation to capture that variability. Thus, as an example only, in past
 398 work, when State Factors were carefully controlled for, relationships between rock material properties and rock fracture properties
 399 were evident from about three to ten meter-scale outcrops per rock type on ridge-forming quartz rich rocks (Eppes et al., 2018).
 400 However, until sufficient magnitude of datasets have been collected for a particular site, the amount of observation area must be
 401 established based on the number of fractures available uniquely at each study site.

402 **4 Selecting fractures for measurement**

403 **4.1 Rules-based criteria for selecting fractures in surface processes research**

404 The term ‘fracture’ is employed with a wide variety of meaning across the geosciences, potentially resulting in large variations in
 405 the range of features that two individuals might study on a single outcrop (Long et al., 2019). Therefore, it is crucial to employ
 406 clear and repeatable rules-based criteria (e.g., Table 1) for what constitute measurable ‘fractures’ within any fracture-related
 407 research. Failing to do so consistently results in a high variance of subjective bias that is more reflective of worker personality than
 408 of the variance in fracture of the outcrop (Andrews et al., 2019). Thus, consistency and documentation are required for deriving
 409 interpretable and repeatable results.

410
 411 The proposed rules (Table 1) for determining which fractures to measure at any given field site were developed in the context of
 412 surface processes research and through iterations with numerous non-expert users (undergraduate students) to arrive at criteria that
 413 provided consistency in observations across users. Because surface processes are frequently and largely dependent both on rock
 414 erodibility and water within a rock body, the recommended criteria are applicable only to open voids, which are known to greatly

415 impact both. Also, because other types of open voids like vesicles are common in rock, additional criteria includes that the open
416 void must be planar in shape, bounded by parallel or sub-parallel sides (hereafter fracture or fracture ‘walls’), with a visible opening
417 that is deeper than it is wide. Fracture walls will pinch together at fracture terminations.

418
419 Voids that fit the shape criteria that are filled with lichens, dust, or other permeable material that can be readily brushed out with a
420 fingernail or prodded with a needle should be included in the dataset. However, it is common for high aspect ratio voids in rock to
421 have been filled with cemented mineral solids during intrusion and metamorphism, diagenesis, or weathering. Fractures, or portions
422 of fractures containing these hardened cements, become the hydrologic and mechanical equivalent of solid rock. Therefore, these
423 zones do not meet the defined ‘open’ criteria and should not be included in the fracture dataset. If such a solid secondary mineral
424 cement forms a discontinuous “bridge” fully connecting the two walls of an otherwise open, planar void, the open length of the
425 fractures on either side of the bridge would be treated as individual fractures. This type of fracture inclusion is common in many
426 settings (see review in Laubach et al., 2019), so a yes/no indication of their presence may be added to the dataset.

427
428 Finally, additional proposed criteria include that the planar void must be continuously open (no ‘bridges’ of cemented mineral
429 material or of rock) for a distance longer than 10 times the characteristic grain size dimension or 2 cm, whichever is greater. In
430 most rock types, this translates to a 2 cm minimum cutoff for countable fractures (Fig. 2a; see Sect. 5.4.1 for measuring lengths).
431 This proposed length threshold is based on three features. First, past work has demonstrated that deriving precise (repeatable)
432 detailed information - other than length - for fractures <2 cm in length is challenging (e.g., Eppes et al., 2010). Second, temperature-
433 dependent acoustic emission measurements (Wang et al., 1989; Griffiths et al., 2017) and theoretical arguments suggest that on
434 single year time scales, fractures on single grain and smaller length scales exist in thermodynamic equilibrium, randomly opening
435 and closing under constant redistribution of ubiquitous diurnal to seasonal thermal stresses within surface rocks. The approximate
436 statistical mechanical ‘rule-of-ten’ states that well-defined equilibrium and nonequilibrium, continuum-scale properties, e.g.,
437 viscosity, density, stress and strain, each determined by myriad microscale random processes, are obtained on length scales
438 approximately 10 times an appropriate molecular length scale, e.g., average atomic size or mean free path length between colliding
439 (gas) molecules. This interpretation is consistent with recommendations for the number of grains the minimum diameter of a
440 sample is for repeatable testing of continuous rock properties such as rock strength and elastic moduli (e.g., ASTM, 2017).

441
442 Last, and practically, the high abundance of fractures below this cutoff significantly increases the time required for fracture
443 measurement. If these smaller fractures are of interest, they can be characterized with photographic analysis (not covered herein)
444 or subjected to semi-quantification via an index (Sect. 5.2).

445
446 Importantly, in some applications, it may be appropriate that a larger minimum threshold in fracture length is chosen. However, in
447 that case, fracture abundances in the rock will possibly dictate that significantly larger observation areas of the rock exposure need
448 to be employed in order to obtain sufficient numbers of fractures to provide representative data (Sect. 4.2).

449
450 Regardless of the threshold length chosen for the study, two adjacent fractures separated by intact rock or bridges of cement are
451 considered two fractures, even if at a distance they appear to be continuous (Fig. 2b). This practice results in repeatable

452 measurement between multiple workers and provides the most accurate representation of past fracture growth and fracture
453 connectivity in the rock body.

454 4.2 Determining how many fractures to measure

455 Most published fracture-focused studies provide no justification for the number of fractures they measure, begging the question -
456 is the dataset representative of the rock body? However, it is a long-recognized concept in fracture and rock mechanics that fracture
457 size distributions are highly skewed and characterized by scale-independent power law distributions (e.g., Davy et al., 2010;
458 Hooker et al., 2014). Thus, the expected power-law distribution of fracture size can be leveraged in most cases to ensure that a
459 representative fracture population has been measured in any given dataset (Ortega et al., 2006).

460
461 Here, it is recommend that to fully characterize the fractures for any site(s), outcrop(s), or feature(s) of interest, sufficient numbers
462 of fractures should be measured such that a statistically robust power-law distribution (p -values <0.01) in fracture length is evident
463 in the data. While other log normal, exponential, and Weibull distributions have been proposed for various fracture datasets (e.g.,
464 Baecher, 1983), employing these distributions depends on preexisting knowledge of the expected dataset. Thus, unless there is
465 prior documentation of fracture distributions at a particular site, the power law distribution should suffice.

466
467 In practice, it is an iterative process to determine the number of fractures required for any given dataset; but generally, on the order
468 of 10^2 fractures are required (e.g., Zeeb et al., 2013) to reach a representative distribution (Fig. 3). When sufficient numbers of
469 fractures have been measured to result in such a distribution, then it can be assumed that the population of measured fractures is
470 representative of all fractures on the rock, outcrop, or group of rocks/outcrops with certain features. For example, if the goal of a
471 study is to test the influence of rock type on fracture width, enough fractures must be measured to allow for a power-law distribution
472 of fracture lengths for *each* of the rock types. That population of fractures can then be considered representative of the given rock
473 type, and statistics on other fracture properties like width can also be reasonably interpreted as representative.

474
475 An example of what that iterative process might look like is found in Fig. 3. In this example, all fractures were measured on the
476 surface of 15-50 cm diameter granitic clasts selected along transects across both a modern wash bar (with few overall fractures per
477 clast) and a ~6 ka alluvial fan bar (with many fractures per clast). For the modern wash, after 5, 30, or 50 clasts, a statistically
478 significant power law distribution is not evident (Fig. 3). However, after 130 clasts, the fit of the power law falls below a p -value
479 threshold of 0.01. Thus, measurements from around 130 clasts were necessary to fully characterize fractures for that particular site.
480 In contrast, the threshold p -value is reached after only 5 clasts for clasts with high fracture number density on the mid-Holocene
481 age site; however, with more clasts examined, more variables per clast can be analyzed in the data. Thus, in order to evaluate
482 different variables (like clast size or shape), the iterative process would repeat, but limiting the analysis to fractures found on clasts
483 meeting the criteria of interest. In this example, a total of 130 clasts per surface were measured, enabling several subsets of data to
484 be examined in order to test the influence on a range of clast properties on fracture characteristics.

485
486 One notable exception to the scale independent power law rule of thumb may be if there are abundant fracture terminations in
487 infilling material. In this case, the size of the fracture (as defined by Table 1) is dictated by the spacing of the filled material bridges.
488 Thus, fracture sets in rocks that contain abundant varnish or secondary precipitates like calcium carbonate may not follow this rule.

489 5 Proposed baseline field data for fracture-focused surface processes research

490 Here, a basic suite of field data (Table 2) is described for all observation areas and all fractures. Table 3 contains a list of
 491 recommended field equipment to make the measurements. The list of data in Table 2 was developed with the goal of allowing the
 492 worker to fully analyze their fracture data in the context of variables known from the literature to influence or reflect fracture in
 493 exposed rocks. Workers may choose to measure only some of these data if, for example, they have controlled for a particular metric
 494 through site or clast selection. As overall knowledge of fractures in surface environments grows, the suggested set of measured
 495 variables should also change, just as, for example, the components of the simple stream power equation have evolved in fluvial
 496 geomorphology literature. The proposed fracture field methods list is also focused on direct ‘observables’ – without interpretation
 497 – that should apply universally across field areas. We readily acknowledge that additional items can and should be added to
 498 accommodate the needs of any specific study.

499
 500 The metrics listed in Table 2 and the associated methods described below are designed to be applicable and translatable to both
 501 natural outcrops and individual clasts. While they may also be applicable to fractures found in quarries and road-cuts, such outcrops
 502 are prone to fracturing that has been anthropogenically induced by blasting, exhumation, and new environmental exposure (e.g.,
 503 Ramulu et al., 2009; He et al., 2012).

504 5.1 The ‘Fracture Sheet’

505 A data collection template is provided that comprises all the proposed standard data, allowing efficient, complete, and detailed
 506 recording of all parameters while in the field (e.g., a “fracture sheet”, Fig. 4 with digital version provided in supplemental data).
 507 The fracture sheet can and should be modified to include additional parameters relative to any study. The template provided here
 508 is structured so that each observation area’s information (e.g., that of each clast, outcrop, or window) shares a row with the first
 509 fracture measured. Then, subsequent rows are employed for additional measured fractures on the same observation area. Each
 510 observation area and fracture are assigned unique identifiers to enable unambiguous reference in subsequent data analysis.
 511 Employing a ‘window’ rather than an entire clast or outcrop as the observation area necessitates slightly different data collection,
 512 so two separate fracture sheets can be found in the supplement.

513
 514 The fracture sheet provides a header space for site meta-data. Any observations that could elucidate the possible contributions of
 515 any State Factor (cl,o,r,p,t,T) acting at the site should be recorded (e.g., the vegetation or topography of the site). This header area
 516 should also be employed to note any and all criteria or conventions used throughout the study. For example, the use of any
 517 convention, such as right-hand rule for strike and dip measurements, should be noted in the header. The criteria employed to select
 518 clasts or outcrops (e.g., their size, composition, etc.) and the nature of the observation areas (e.g., only the north face of all clasts;
 519 or entire exposed clast surface for all outcrops) should also be noted.

520 5.2 The use of semi-quantitative indices

521 It is recommended that indices be employed for many observations following similar existing semi-quantitative methods
 522 commonly employed in both soil sciences (e.g., Soil Survey Staff, 1999) and sedimentology (e.g., rounding and sorting). The use
 523 of indices, rather than precise measurements, is especially appropriate for fractures and fracture characteristics given the natural

524 variation between different rocks. Also, high numbers of small or discontinuous features on rock surfaces frequently precludes
 525 their accurate counting within a reasonable amount of time; for example, counting all fractures <2 cm in length.

526
 527 Two particularly useful generic ‘abundance’ indices are defined here that are similar to those employed for quantifying the
 528 abundance of roots and pores in soils (Schoeneberger et al., 2012), whereby the quantity or coverage of specific elements or features
 529 is estimated within a specified area. For both, a ‘frame’ is employed whose size is dependent on the size of the feature being
 530 observed (Fig. 5). Features that are ≤ 0.5 cm are observed in 1 cm² frames; features >0.5 to <2 cm are observed in a 10 cm² frame;
 531 and features ≥ 2 cm are observed in a m² frame. Cut-out stencils of these sizes may be constructed and employed. The observer
 532 imagines randomly placing the ‘frame’ several times on any given portion of the observation area, noting the abundance of the
 533 feature of interest within the frame. The indices are based on the average value of abundance observed in any given such ‘frame’
 534 across the entire area of observation (e.g., the entire clast, the entire outcrop, or the outcrop window).

535
 536 The first index scales from 0 to 4 and is applicable for ‘countable’ features of interest in the research like small fractures, fossils,
 537 or large phenocrysts. The index is: none – 0 (no visible features in any frame), few -- 1 (<1 feature on average), common -- 2 (≥ 1
 538 and <5 features on average), very common -- 3 (≥ 5 and <10 features on average), and many -- 4 (≥ 10 features on average).

539
 540 The second index scales from 0 to 5 and is employed for features that are not readily counted nor consistent in size (like lichen,
 541 varnish, fine grained mafic, or felsic minerals). In these cases, the index is based on the percentage of the rock surface covered by
 542 the feature: none – 0; very little – 1 (<10%); little – 2 (≥ 10 and <30%); common – 3 (≥ 30 and <60%); very common – (≥ 60 and
 543 <90%); and dominant – 5 ($\geq 90\%$). A percentage estimator (Fig. 6) should always be employed to assign the index categories –
 544 even experienced field workers are subject to ‘quantity bias’.

545 5.3 Measuring rock characteristics

546 The following rock characteristics should be measured for each observation area – each clast, outcrop, and/or window – that is
 547 employed in a study. Some fracture characteristics not captured in individual fracture measurements are also included. In particular,
 548 fracture connectivity and fracture spacing should be measured after all individual fractures within the observation area have been
 549 identified and measured.

550 5.3.1 Clast, outcrop, or window dimensions

551 Rock – or outcrop – size, aspect, and slope can impact stress-loading through, for example, thermal stress distribution (e.g., Molaro
 552 et al., 2017; Shi, 2011). Or, for instance, natural outcrop height has been linked to its exposure age and/or erosion rates (e.g.,
 553 Hancock and Kirwan, 2007). The dimensions of the clast, outcrop, or window employed for fracture observations are also required
 554 for calculations of fracture number density and intensity (i.e., the number/length of fractures per unit area; see Sect. 6.1).

555
 556 The length and width of planar ‘windows’ are measured directly. If a window ‘bends’ across multiple faces of the rock surface,
 557 then separate length and width measurements should be made for each face with a distinct aspect. These areas are then added
 558 together for fracture number density and intensity calculations.

559

560 The vast majority of rock clasts and outcrops found in nature have ‘cuboid’ forms (Domokos et al., 2020). Thus, length, width,
 561 and height of individual clasts or outcrops may be reasonably employed to calculate the exposed surface area (see Sect. 6.1 for
 562 calculations). If clasts or outcrops are well-rounded, spherical or half-spherical surface areas can be employed, depending on burial.

563
 564 For all dimension measurements regardless of rock shape, metrics are measured as point-to-point orthogonal measurements. Length
 565 is measured parallel to the longest axis. Width is measured on the widest extent that is perpendicular to length, and height is
 566 measured vertically from the uppermost surface of the rock down to the ground surface. If a through-going fracture splits the rock
 567 into two pieces that remain *in situ*, it should still be considered one rock and measured accordingly. If a clast or outcrop is spheroidal
 568 in shape, that should be noted for future surface area calculations.

569
 570 For site preservation, and to minimize geoheritage and environmental impacts, rocks should not be moved from their natural state;
 571 therefore, the height measurement of a highly embedded rock will only represent the height of the exposed rock surface above the
 572 ground. A metric derived to estimate the degree to which clasts are exposed versus embedded is provided in Sect. 5.3.8.

573 5.3.2 Sphericity and roundness

574 Sphericity and roundness from standard sedimentology practices (e.g., Krumbein and Sloss, 1951) provide metrics for rock shape.
 575 Shape can influence stress distribution in a mass and, therefore, rock fracture. For example, generally, corners tend to concentrate
 576 stresses, and ‘corner fractures’ are a recognized phenomenon in fracture mechanics (e.g., Kobayashi and Enetanya, 1976). Thus,
 577 this metric has been included as one to be measured both for outcrops and for clasts.

578
 579 Sphericity refers to the length by width ratio, or elongation, of the clast or outcrop, whereas roundness is a measure of angularity
 580 (Fig. 7). The roundness and sphericity designation for the square on the chart in Fig. 7 most closely matching the dominant shape
 581 of the entire clast or outcrop should be noted (ex. r-SR; s-SE). If a more precise rock shape analysis is needed, a modified Kirkbride
 582 device can be used to quantitatively measure rock roundness (see Cox et al., 2018 for device modifications and methodology).

583 5.3.3 Grain size

584 Mean grain size can impact numerous fracture and stress characteristics including the proclivity for granular disintegration
 585 (Gomez-Heras et al., 2006), fracture toughness (Zhang et al., 2018), initial fracture length, thermal stress disequilibrium (Janio De
 586 Castro Lima and Paraguassú, 2004), and bulk elastic properties (Vazquez et al., 2015). The mean grain size should be visually
 587 estimated by comparing the dominant size of individual grains or mineral crystals to a standard grain size card. This size can be
 588 reported as one average value for all minerals, or different values for different suites of minerals (e.g., felsic vs. mafic), depending
 589 on the lithological assemblage(s) of the observation area(s).

590 5.3.4 Fabric and fracture filling

591 Here, the term ‘fabric’ is employed to refer to any preexisting (prior to weathering) primary or diagenetic planar, linear, or randomly
 592 oriented anisotropies within the rock comprising the outcrop or clast of interest. Fabric is most commonly observed as fossils or
 593 lithological bedding planes in sedimentary rocks and as crystal horizons or foliation structures in igneous or metamorphic rocks.
 594 Also, all rocks can have diagenetic mineral deposits within parts of otherwise open fractures or contain fully filled veins and dikes.

595 Finding mineral deposits in open fractures points to a deeper origin. Rock fabric can impart anisotropy that influences rock strength,
 596 fluid flow, and fracturing clustering, rates, and orientations (e.g., Nara and Kaneko, 2006; Zhou et al., 2022). Thus, any visible
 597 fabric type, as well as the strike(s) and dip(s) (or trend(s) and plunge(s)) of each parallel or subparallel set should be noted in the
 598 fracture sheet for each observation area. By collecting these data, it can be determined by comparing orientations the extent
 599 fractures in the dataset are influenced by these fabrics.

600 5.3.5 Fractures <2 cm in length

601 Fractures <2 cm in length can comprise a significant portion of all fractures on a given rock exposure, particularly in coarse
 602 crystalline rock types (e.g., Alneasan and Behnia, 2021). Thus, it is recommended that an index is recorded, using an observation
 603 ‘frame’ (see Sect. 5.2) that quantifies the abundance of fractures less than 2 cm in length (hereafter ‘small fractures’).

604
 605 The approximate number of small fractures visible each time the ‘frame’ is moved should be observed. A rough average of all
 606 theoretical frames should be taken, and the categories in Fig. 5 should be used to assign an abundance. For example, if there are
 607 generally either zero or one small fracture in any given 10 x 10 cm frame, the abundance would be “1” – i.e., few, <1 per unit area.

608 5.3.6 Granular disintegration

609 Granular disintegration refers to evidence of *active* loss of individual crystals or grains due to fracturing along grain boundaries
 610 (i.e., sedimentary particles or igneous or metamorphic crystals). This feature is observed on the rock surface as individual grains
 611 or small clusters of grains of the rock that can be brushed away by hand. Granular disintegration is commonly observed in coarse
 612 igneous, metamorphic, and sedimentary rocks, and over the long-term leads to the accumulation of sediment comprised of
 613 individual crystals or small clusters of a few crystals on the ground surface (Eppes and Griffing, 2010; Isherwood and Street, 1976;
 614 Gomez-Heras et al., 2006).

615
 616 This disintegration comprises the complete separation of intergranular fractures. Because the fractures that comprise granular
 617 disintegration are typically too small to be readily measured in the field, however, its presence is assumed when loose grains are
 618 present on the rock surface. The worker should mark affirmatively (circling the ‘G’ on the Fracture Sheet) if there is evidence of
 619 granular disintegration on the rock surface of observation. If more detail is desired, an abundance index (e.g., Fig. 5) may be
 620 employed to quantify what percentage of the surface of observation contains loose grains.

621 5.3.7 Pitting

622 Pitting is the occurrence of small holes or fissures that form on the rock surface due to granular disintegration or to preferential
 623 chemical weathering of certain mineral types, typically feldspars and micas in silicate rocks. Pitting is distinct from granular
 624 disintegration as it is not necessarily ‘actively’ occurring – i.e., pitting can exist without loose grains on the rock surface. It is
 625 included here as a rock property because of its possible linkage to intergranular fracturing. Furthermore, measuring the extent and
 626 depth of pitting due to chemical weathering has long been employed as a relative age dating tool in Quaternary geology applications
 627 (Burke and Birkeland, 1979).

628

629 Pitted surfaces form as individual grains become weathered and fall out or are dissolved; or, for soluble rocks like carbonates, as
 630 entire rock regions are dissolved. Pitting can either be quantified as present/absent (circling P on the fracture sheet) or as a quantity
 631 index (Figs. 4 and 5).

632 5.3.8 Clast exposure

633 This metric is used to record to what degree individual clasts appear to be exposed above the ground surface. Individual clasts are
 634 known to weather and erode from the upper rock surface down until they become ‘flat’ rocks at the ground surface (e.g. Ollier,
 635 1984). Surface exposure can be estimated as the amount and shape of a boulder’s exposed surface that is currently not covered by
 636 loose sediment, vegetation, or other material. This exposure is grouped into four categories: 0 - the clast is sitting above the ground,
 637 and its sides curve downward toward the ground surface almost meeting; 1 - the clast is partially covered, with sides curving
 638 downward toward the ground surface but not meeting; 2 - the clast is “half” covered, with sides projecting roughly vertically into
 639 the ground surface; 3 - the clast has only one upward facing side visible at the ground surface. In a field study, a correlation test
 640 on data from 300 boulders revealed a positive correlation of 0.66 between the indices and the fraction of boulder embeddedness
 641 (in vertical length) (Shaanan et al., 2022).

642 5.3.9 Lichen and varnish

643 Lichens and other plant life can act to push rocks apart during growth (Scarciglia et al., 2012), but have also been shown to
 644 strengthen rocks through infilling of voids or shielding from stress-inducing sunlight (Coombes et al., 2018). It is noted that lichen
 645 are living organisms that would be killed by removal. In order to determine if a lichen-coated lineation is in fact a measurable
 646 fracture (see Sect. 4.1), a needle or straight pin may be employed to poke through the lichen into the possible void of the fracture.
 647

648 Rock varnish (oxide staining that can appear as a dark gray/black or orange coating on rock and typically contains Fe or Mn oxides)
 649 is well-documented to evolve over time. The extent of varnish cover has been employed frequently as a relative-age indicator,
 650 particularly in arid environments (e.g., Mcfadden and Hendricks, 1985; Macholdt et al., 2018). Thus, variations in varnish across
 651 the rock face can provide evidence of loss of surface material through *in situ* fracturing.
 652

653 Lichen and varnish can come in many forms and be difficult to distinguish from each other and from primary rock minerals, hiding
 654 in fractures, pitting holes, and atop mafic crystals. So, careful consideration of the types of lichen and varnish that may be found
 655 in field sites and close inspection with a hand lens is recommended. A fresher exposure of the rock surface can help in the
 656 identification of lichen and varnish relative to the natural rock composition and color. Due to the geodiversity impact, however,
 657 such exposures should not be made with force.
 658

659 The quantity of lichen and varnish (secondary chemical precipitates deposited on the subaerial rock surface) visible on the rock
 660 observation surface are separately estimated using a visual percentage estimator (Fig. 6) and a quantity index is assigned (Fig. 5;
 661 Sect. 5.2).
 662

663 5.3.10 Collecting samples for microfracture analyses

664 Rock microfractures (those not visible with hand lens in the field) play a central role in contributing to rock strength, anisotropy,
 665 and subsequent macrofracturing processes (Kranz, 1983). It is beyond the scope of the field-based methods presented herein to
 666 describe microfracture measurement and analysis, which continues to evolve (e.g., Griffiths et al., 2017; Healy et al., 2017).
 667 Instead, suggestions for rock sampling and placement of thin-section billets are provided.

668
 669 Thin-section analysis of microfractures is a time-consuming process, particularly when considering the per-capita rock volume
 670 examined. It is therefore extremely important to select rock or portions of rock that are precisely the rock type of interest. For loose
 671 clasts, an entire clast can be sampled and a thin-section billet processed in the lab. For larger clasts and bedrock, a smaller portion
 672 must be extracted. By sampling pieces that are already naturally detached, or nearly detached, fracturing that arises due to chiseling
 673 or hammering is avoided.

674
 675 For both clasts and outcrops, the natural orientation of the sampled rock (its horizontal and azimuthal directions) should be marked
 676 on the specimen. The sample should be photographed prior to removing from its location. It is essential to ensure all permitting is
 677 in place prior to sampling.

678
 679 Similar to clast or outcrop selection, care must be taken when considering the location within the rock that the thin-section billet
 680 will be cut. Because microfracture strike and dip can be influenced by environmental, gravitational, and tectonic forces, both the
 681 depth and orientation of the billet should be noted and controlled for as appropriate for all samples compared within a single study.

682 5.3.11 Fracture connectivity

683 Fracture connectivity has long been recognized as being key to rock strength and fluid flow (e.g., Rossen et al., 2000; Long and
 684 Witherspoon, 1985), and presumably contributes to rock erodibility given that fractures must intersect for rock to erode. There is
 685 a large body of literature that addresses fracture connectivity and how to measure it (e.g., Berkowitz, 2002; Barton et al., 1993;
 686 Healy et al., 2017; Sanderson and Nixon, 2018), especially in the context of reservoirs and rock quality index studies. As yet,
 687 fracture connectivity has been little studied in the context of surface processes, but likely holds high potential given its relationship
 688 to water access and to erodibility. Here, the focus is on a simple, rules-based observation of fracture intersection ‘nodes’ (e.g.,
 689 Barton and Hsieh, 1989; Manzocchi, 2002; Forstner and Laubach, 2022; Sanderson and Nixon, 2018) that comprise the basis for
 690 fracture network connectivity assessment (e.g., Andresen et al., 2013).

691
 692 After all fractures within each observation area have been identified and measured (Sect. 5.4), all fracture links within the
 693 observation area should be counted and recorded by noting their relationship to other fractures (Fig. 8): dead end (I-node),
 694 crossing (X-node), and/or abutting without crossing (Y-node). Numbers of nodes per area can then be used as a proxy for
 695 fracture connectivity. If fracture connectivity is of particular interest for the research, rules-based ‘contingent mode’ (C-node)
 696 intersections may also be added (Forstner and Laubach, 2022). An example of a C-node rule might be if fractures >100 mm in
 697 length terminate within 10 mm of another fracture, its termination would be a c-node. Another C-node definition could comprise
 698 intersection relations where visible connected traces are sealed with secondary minerals. These c-nodes may be important when
 699 there are ambiguous at-depth relationships between fracture terminations (e.g., Fig. 2b).

700 701 5.3.12 Fracture spatial arrangement

In addition to overall fracture density and intensity, the arrangement of fractures in relation to each other (e.g., evenly spaced, random, clustered in space) can impact loci of rock mass weakness, fluid flow, and landscape morphology. Laubach et al. (2018) is a special edition of the *Journal of Structural Geology* devoted to spatial arrangement of fractures. The mathematical analysis of clustering is beyond the scope of this field guide, however, measuring one-dimensional fracture spacing along scan lines can be used in many such calculations (Corrêa et al., 2022; Marrett et al., 2018).

Following similar methods as those used for locating windows (Sect. 3.4), lines should be established across the center of observation area, perpendicular to each other in order to capture different orientations of fractures. A tape is then laid across the lines, and, beginning with the edge of the observation area as distance 0, the distance along the tape of each fracture is noted, as well as the “Crack ID” already established for that fracture on the Fracture Sheet. If fractures are marked with chalk, this is an easy process. In that way, the size of each fracture and its adjacent spacings is noted. Fracture arrangement is scale dependent. These spatial arrangement data can go on the back of the Fracture Sheet.

5.4 Individual fracture characteristics

The following properties are measured for each fracture found within the observation area that meets all the fracture selection criteria listed in Table 1. In order to keep track, it is useful to mark fractures with chalk within the observation area after you have made their appropriate measurements.

5.4.1 Length

Fracture length is measured for the entire surface exposure length of the fracture; i.e., around corners and up and down rock topography (Fig. 2a). Measurements can be made with flexible seamstress tape to follow the curve of a fracture’s exposure on the rock surface. Length is only measured where there is an open void (Fig. 2b; Sect. 4.1), because to measure across bridges of secondary cemented material or rock would be to infer future fracture propagation that has not yet occurred. By only measuring the open portion of voids, the user avoids arbitrary interpretation of possible behavior. Thus, if a seemingly continuous fracture (Fig. 2b, left inset) is in fact separated by bridges of solid rock (Fig. 2b, right inset), then these should be measured as two different fractures and their lengths should terminate at the rock bridges. The inset in Fig. 2b reveals four fractures possibly meeting all Table 1 criteria. If two fractures intersect in x- or y-nodes (Fig. 8), each fracture is defined by its own distinct strike, and the full length of the full open fracture with that strike is measured (e.g., the length of segments ab and cd in Fig. 8).

Importantly, when using a ‘window’ approach to rock observation area, both the total length of the fracture extending beyond the window, as well as the total length within the window, should both be recorded. The latter is employed in fracture intensity calculations (Sect. 6.1); the former provides representative information about all fracture lengths on the rock being measured.

5.4.2 Width

Fracture aperture widths (hereafter, ‘widths’) can impact both the strength and permeability of rock. Generally, they scale with fracture length and, thus, can possibly reflect the innate subcritical cracking parameters of the rock (Olson, 2004). Fracture widths typically vary along their exposure and pinch out at fracture tips. Determining an average or representative width within a single fracture can thus be somewhat arbitrary and subject to bias. Locating the widest aperture is less subject to bias and can also provide

737 information about fracturing processes. Also, the center of the open fracture is an objectively repeatable location, and also where
 738 the fracture might be expected mechanistically to be the widest. However, given that this relationship can become complicated as
 739 fractures fill or branch, it is recommended here that recording fracture width both at the midpoint of the measured length of the
 740 exposed fracture be consistent as well as recording its maximum width along its exposure.

741
 742 Both measurements should only be made in regions of the fracture where fracture walls are parallel or sub-parallel (e.g., green
 743 arrows in Fig. 9), avoiding locations where fracture edges have been obviously rounded by erosion or chemical weathering, or
 744 where large pieces have been chipped off or are missing (e.g., red arrows in Fig. 9). If it is unclear if a portion of the fracture has
 745 chipped off (e.g., orange arrow in Fig. 9), a notation can be made and employed later to eliminate potential outliers in the dataset.
 746 Fractures greater than about 3 mm in width can be easily measured by inserting the back-blades of digital calipers into the widest
 747 opening of the fracture. For narrower fractures, a logarithmically binned ‘crack comparator’ (Fig. 7) is recommended (Ortega et
 748 al., 2006), whereby the line on the comparator most closely matching the fracture aperture is chosen.

749 5.4.3 Strike and dip

750 Fracture orientation (i.e., strike and dip) is a function of the orientation of existing anisotropy within the rock and the orientation
 751 of the principle stresses that drove its propagation. Fracture orientations are commonly related to tectonic forces; however, both
 752 gravitational and environmental stresses can also be directional (e.g., St. Clair et al., 2015; Mcfadden et al., 2005). When fractures
 753 are growing at subcritical rates, they can lengthen through a series of ‘jumps’ that link parallel or subparallel smaller fractures. The
 754 following suggestions are for research aimed not at characterizing these small mm-cm scale heterogeneities, but rather identifying
 755 major stresses and heterogeneity in the entire rock body.

756
 757 Fracture orientation is measured with a geological compass or similar tool that has both azimuthal direction and inclinometer
 758 functionality. When measuring strike and dip of fractures, it is important to visualize how the fracture plane intersects the rock
 759 surface, as if slipping a sheet of paper into the ‘file folder’ of the fracture. For larger fractures, weathering and erosion may have
 760 resulted in loss of rock along the upper edge of the fracture, so it is imperative to measure the angle at the interior of the fracture
 761 where its walls are parallel (Fig. 9) to avoid measuring instead the angle of the eroded face.

762
 763 Fractures grow until they intersect other fractures and/or branch. If fractures appear to intersect or branch (i.e., two connected
 764 planar voids with noticeably different orientations joined by a sharp angle), their lengths should be measured separately as well as
 765 their orientations (e.g., two strikes and dips) as previously mentioned. For fractures that meander around mm-cm scale
 766 heterogeneities like phenocrysts or fossils, the overall trend is measured. A 1 to 10 rule of thumb can be used whereby, as long as
 767 the ‘jog’ in the fracture orientation is $<1/10$ of the fracture length, it is not measured.

768
 769 Fracture tip propagation direction may also slowly change as the orientation of external stresses or internal stress concentrations
 770 change withing the rock mass. For curvilinear fractures, the average orientation can be measured, as the orientation of the non-
 771 curved plane whose ends are defined by the ends of the fracture. Alternatively, the fracture curvilinear plane may be subdivided
 772 into roughly linear planes and each orientation measured. If this latter approach is taken, the intersection should be marked as a
 773 node, and two lengths recorded. It is important to note which method was employed and to remain consistent for all measurements.

774

775 There are numerous commonly-employed conventions for measurements of strike and dip. If the worker is consistent and clear in
 776 the use of their preferred convention and in the presentation of their data, any are acceptable. If the worker has no such prior habits,
 777 record strikes as an azimuthal orientation from 0-359 degrees, and dip angle as an angle deviation from horizontal of 0-90 degrees.
 778 For dip direction, a convention such as the “right-hand rule” should be employed whereby the dip direction is always known from
 779 the orientation of the strike alone. For example, the right-hand rule states that the down-dip direction is always to the “right” of the
 780 measured and recorded strike when the observer is facing the same direction of the strike. Therefore, the strike that is recorded is
 781 the one whereby the dip direction is always +90 degrees clockwise (to the right) from the strike direction.

782 5.4.4 Fracture parallelism

783 Noting the parallelism of the fractures can help to better understand the origins of the population of fractures at a site. Parallelism
 784 is common because fractures often follow rock heterogeneities or anisotropies such as bedding, foliation, veins, or even the rock
 785 surface. Fractures in a single bedrock outcrop or clast are also commonly parallel because they have formed due to external stress-
 786 loading with a consistent orientation (e.g., those related to tectonics or directional insolation). Thus, noting parallelism may help
 787 to distinguish the origins of fractures, though not always. For example, ‘surface parallel fractures’ (e.g., Fig. 2a) - commonly
 788 referred to as exfoliation, sheeting joints (e.g., Martel, 2017), or spalling – vary dramatically in scale and can have origins related
 789 to several different factors including tectonic-topographic interactions (Martel, 2006), chemical weathering and volumetric
 790 expansion (Røyne et al., 2008), and thermal stresses related to insolation (e.g., Lamp et al., 2017; Collins and Stock, 2016) and fire
 791 (e.g., Buckman et al., 2021).

792

793 In the fracture sheet, features to which the fracture is parallel should be documented. A visual inspection will suffice for most
 794 applications, but for applications where more precision is needed, the fracture may be considered parallel if the strike and dip of a
 795 fracture is within $\pm 10^\circ$ of the orientation of the feature (the rock’s long axis, its fabric, or its outer surface). A fracture may be
 796 parallel to more than one feature in the rock. Categories may be added as necessary for rocks with other repeating features unique
 797 to the field site (fossils; veins, etc.).

798 5.4.5 Sheet height

799 Surface parallel fractures naturally detach ‘sheets’ of rock between the fracture and the rock surface (‘h’ in Fig. 2a). The thickness
 800 of these sheets may be of interest for understanding the size of sediment produced from the fracture or for understanding the
 801 stresses that produced the fracture. Sheet height is measured using calipers at the location of the maximum height of the sheet and
 802 is only used for surface parallel fractures. To limit these measurements to those that have likely formed in situ as related to the
 803 current morphology of the rock, a rule of thumb is to only measure those ‘sheets’ that would result in removal of $<10\%$ from the
 804 outer surface of the rock downward into the dimension(s) of the rock face(s) to which they are perpendicular.

805 5.4.6 Weathering index

806 Rock fracture is ultimately a molecular scale bond-breaking process; so, when fractures propagate, they initially form a razor-sharp
 807 lip or edge. Over time, these edges naturally round through subsequent chemical and physical weathering, erosion, and abrasion
 808 (e.g., regions of the red arrows in Fig. 9). Following similar research that has demonstrated time-dependent changes in rock surface

809 morphology due to such weathering processes (e.g., Shobe et al., 2017; Gómez-Pujol et al., 2006; McCarroll, 1991), we established
810 an index of relative degree of such rounding along a fracture edge to be noted in the fracture sheet:

- 811
812 1: fresh with evidence of recent rupture (flakes/pieces still present, but not attached)
813 2: sharp, no rounded edges anywhere
814 3: mostly sharp with occasional rounded edges
815 4: mostly rounded edges with occasional sharp edges
816 5: all rounded edges
817

818 6 Suggestions for data analyses

819 For initial data exploration, normal cross-plots, or quantile-quantile plots, as well as standard correlation analysis may be applied
820 to rock and fracture data. For categorical data, normal analytical techniques (histograms, discrete correlation analysis, etc.) can be
821 applied. As with all heavy-tailed data, the median is preferred over the mean value to understand a characteristic value—though
822 power distributed data generally does not have a characteristic dimension. Standard statistics such as mean, variance, skewness,
823 and kurtosis all remain valid to explore and evaluate the datasets.

824 To understand fracture length and fracture width data, it is key to first recognize that, with the exception of studies such as in rocks
825 with fractures with uniform spacing and bedding-controlled widths (Ortega et al., 2006), the data will have a heavy-tailed
826 distribution, such as lognormal, gamma, or power law. As mentioned above, of these, strong observational and theoretical evidence
827 suggests that fracture size is most commonly power law distributed (e.g., Bonnet et al., 2001; Davy et al., 2010; Hooker et al.,
828 2014; Ortega et al., 2006; Zeeb et al., 2013), i.e.,

$$829 \quad n(b) = Ab^{-\alpha} \quad (1)$$

830 where b is the fracture dimension (length or width) of interest, n is the number of fractures with dimension d , and A and α are
831 constants. When log-transformed, Eq. (1) becomes

$$832 \quad \log(n(b)) = \log(A) - \alpha \log(b) \quad (2)$$

833 which has led many practitioners to fit Eq. (2) by linearly binning the data in n , then log-transforming the data and fitting the
834 resulting data with a linear regression. This has proven to lead to significant bias in estimates, $\hat{\alpha}$, of the power law exponent
835 (Bonnet et al., 2001; Clauset et al., 2009; Hooker et al., 2014) and is not recommended despite its common usage.

836 Two straight-forward approaches have been shown not to have biases, or misestimates of the exponent α . 1) The following is based
837 on Clauset et al. (2009). First, the exponent can be found from the cumulative distribution of the dimensions, $C(b)$, or number of
838 fractures with dimension greater than b , i.e.,

$$839 \quad C(b) = \int_b^{b_{\max}} n(b) db \quad (3)$$

840 Where b_{\max} is the maximum size of the fracture dimension (e.g., maximum length or width). The cumulative power law distribution
841 has the form

842
$$C(b) \propto b^{1-\alpha} \quad (4)$$

843 It is common to denote $1-\alpha$ as c . To find α (or c), the dimension data is logarithmically binned. In other words, the dimension data
 844 is binned on a logarithmic (1, 10, 100, ...) frequency scale, and then log-transformed. At this point, linear regression techniques
 845 can be applied to estimate α and assess uncertainty. However, in all cases, uncertainty estimates such as R^2 will overestimate the
 846 certainty for such log-transformed data; but at least the estimate of α is unbiased.

847 2) Another method to find α from a data set of fracture dimensions is to use the maximum likelihood estimator (MLE) given by

848
$$\hat{\alpha} = 1 + N \left[\sum_{i=1}^N \ln \left(\frac{b_i}{b_{\min}} \right) \right]^{-1} \quad (5)$$

849 where $\hat{\alpha}$ is the estimate of the exponent in (1), b_i is the dimension of the i th fracture, b_{\min} is the minimum valid fracture dimension
 850 (see below) and N is the total number of samples (Clauset et al., 2009; Hooker et al., 2014). The MLE estimate has the advantage
 851 of an accurate estimate of standard error, σ , given by

852
$$\sigma = \frac{\hat{\alpha}-1}{N} + O\left(\frac{1}{N}\right). \quad (6)$$

853 Clauset et al. (2009) showed that both the logarithmically-binned cumulative distribution and the MLE estimator produce unbiased
 854 estimates of the exponent. For all empirical power law distributions, there is a scale; in this case b_{\min} , below which power law
 855 behavior is not valid. This can be visually assessed by plotting Eq. 2 with logarithmically binned n . The interval between b_{\min} and
 856 b_{\max} where the slope is linear is where the power law is valid (Clauset et al., 2009; Ortega et al., 2006), and Clauset et al. (2009)
 857 presents a formal method to find b_{\min} and b_{\max} . Hooker et al. (2014) use a χ^2 test to evaluate the goodness of fit, which is simpler
 858 than the p-tests of the Kolmogorov-Smirnov statistic proposed by Clauset et al. (2009).

859 6.1 Fracture number density and fracture intensity

860 Here, following large portion of fracture mechanics literature and for clarity, the term ‘fracture number density’ is employed to
 861 refer to the number of fractures per unit area (e.g., # fractures/m²), and the term ‘fracture intensity’ to the sum length of all fractures
 862 per unit area (e.g., cm/m²). However, it is crucial to note that these terms are frequently defined differently and in inconsistent
 863 ways across disciplines and even within disciplines (e.g., Barthélémy et al., 2009; Narr and Lerche, 1984; Ortega et al., 2006;
 864 Dershowitz and Herda, 1992). It is imperative that workers clearly define their usage in each work.

865
 866 In the suggested use herein, the ‘area’ refers to the surface area of observation area. For fractures measured in ‘windows’ (Sect.
 867 3.4), the length of fractures only *within* the window is used, and the area of the window (e.g., 10 cm x 10 cm) for the calculations.
 868 For loose clasts and outcrops, the appropriate calculation of surface area will depend on the shape and angularity of the rock. For
 869 most rocks, calculations for the surface area of the exposed sides of a rectangular cuboid ($L*W + 2*(L*H) + 2*(W*H)$) are
 870 appropriate.

871 6.2 Circular data

872 Standard 'linear' statistics cannot be employed for circular data. Instead, circular statistical and plotting software can be used for
 873 the visualization and analysis of strike and dip data. The statistics employed by such software is typically based on established
 874 circular statistical research methods (e.g., Mardia and Jupp, 1972; Fisher, 1993). The following statistics are useful in reporting
 875 strike and dip data.

876
 877 The Mean Resultant Direction (a.k.a. vector mean, mean vector) is analogous to the slope in a linear regression. Circular variance
 878 can be quantified using either a Rayleigh Uniformity Test (for single mode datasets) or a Rao Spacing Test (for datasets with
 879 multiple modes), whereby p-values <0.05 indicate non-random orientations. If p-values for these tests are below a threshold (e.g.,
 880 <0.05), then data are considered non-uniform or non-random.

881
 882 The Rayleigh statistic is based on a von Mises distribution (i.e., a normal distribution for circular data) of data about a single mean
 883 (i.e., unimodal data). Therefore, for multi-modal data, the variance might be high, but nevertheless, the data might be non-uniform.
 884 The Rayleigh Uniformity Test calculates the probability of the null hypothesis that the data are distributed in a uniform manner.
 885 Again, this test is based on statistical parameters that assume that the data are clustered about a single mean.

886
 887 Rao's Spacing Test is also a test for the null hypothesis that the data are uniformly distributed; however, the Rao statistic examines
 888 the spacing between adjacent points to see if they are roughly equal (random with a spacing of $360/n$) around the circle. Thus,
 889 Rao's Spacing Test is appropriate for multi-modal data and may find statistical significance where other tests do not.

890 8 Case example

891 To demonstrate the consistency of results that might be achieved across users, we provided minimal training (one demonstration
 892 with some minor oversight of initial work) to four groups of two students each. The fifth pair of workers included a scientist who
 893 had logged over 500+ hours of experience using the standardized methods. Each of the five groups followed the methods to
 894 measure the length and abundance of fractures on boulders (15-50 cm max diameter) on the same geomorphic surface (a 6000-
 895 year-old alluvial fan in Owens Valley California, comprised of primarily granitic rock types). Each group followed the methods
 896 described herein for rock and fracture selection and measurements. As such, the results from each group (Fig. 10; Data Supplement)
 897 could be compared not only for fracture selection and measurements, but also for observation area selection – a key component of
 898 collecting data that is representative of a particular site.

899
 900 We find that the data collected by each of the groups for fracture length, number of fractures per rock, and rock size are statistically
 901 indistinguishable by student t-test (all pairs of p-values > 0.1 ; Fig. 10; Data Supplement). Also, there is no consistent difference
 902 between measurements made by the novice groups and that of the trained group. The mean fracture lengths from the four novice
 903 groups novice group (37 ± 23 mm to 59 ± 51 mm) span across that of the mean collected by the well-trained group (42 ± 22 mm;
 904 Supplement), as do the number of fractures per rock (2 ± 2 to 6 ± 8 for novice groups compared to 3 ± 3 for trained group). With only
 905 one exception (fracture length for Group 1), variance between groups does not range by more than a factor of 3 in any of the data
 906 – a common rule of thumb for the threshold of 'similar' variance between small datasets. Overall, especially given the relatively
 907 small size of the datasets (~ 10 -20 rocks and ~ 40 -60 fractures each), this comparison suggests that the results using the standardized
 908 methods are reproducible, even with novice workers with minimal training.

909 9 Conclusions

910 The methods proposed herein comprise a ‘first stab’ at standardization of field data collected in rock fracture research surrounding
911 surface processes and weathering-based geologic problems. The outlined methods comprise best practices derived in large part
912 from existing work in the context of structural geology and fracture mechanics. They also comprise general guidance and nuances
913 developed from experiences (and mistakes) over the last two decades of fracture-focused field research applied to geomorphology
914 and soil science. It is our hope that providing these rules-based, detailed, accessible, standardized procedures for gathering and
915 reporting field-based fracture data will open the door to rapidly building a rigorous galaxy of new datasets as these guidelines and
916 methods become more widely adopted. In turn, they may enable future workers to better compare and merge fracture data across
917 a wide range of studies, permitting future refinements of our understanding of rock fracture and in the methods themselves.
918 Compiling such a standardized global dataset is the best hope for fully characterizing the role and nature of fractures in Earth
919 surface systems and processes.

920 10 Author Contributions

921 MCE spearheaded the evolution of the development of the guiding principles and methods described herein as well as writing of
922 the manuscript. JA, SB, MD, SE, FM, SP, MR, and US all participated extensively in field campaigns during which the methods
923 were developed and refined, and they contributed to editing of manuscript and editing and development of figures. MM, AR and
924 RK contributed to the development of theoretical statistical analyses practices that are outlined in the document and the editing of
925 the manuscript.

926 11 Competing interests

927 The authors declare that they have no conflict of interest.

928**929 12 Data Availability****930**

931 All data presented in the manuscript are available in the Supplement.

932 13 Acknowledgements

933 The body of knowledge presented herein was derived in large part over the course of research funded by the National Science
934 Foundation Grant Nos. EAR#0844335 (with supplements #844401, #0705277), #1744864, and #1839148 and NASA ROSES
935 Mars Data Analysis Program award #NNX09AI43G. Several photographs in figures were cropped and employed with permission
936 from Marek Ranis, Artist-in-Residence for NSF #1744864. We thank Caire Bossennec and Steven Laubach for their constructive
937 reviews. Laubach especially contributed significantly to the revised version of the manuscript. In addition, the authors wish to
938 acknowledge the contributions from countless undergraduate and graduate students who contributed to the application and
939 development of these methods in classes taught by MCE at the University of North Carolina at Charlotte.

940**941****942**

Figure Captions

Fig. 1. Images illustrating the selection of observation areas for clasts and outcrops. A. Photograph of a transect established for clast selection. Black dot: predefined transect interval location on the tape. Red dot: clast that does not fit the predefined clast selection criteria (e.g., it is too big). Green dot with red circle: clast that fits criteria but is further away from the interval point than the clast with the green dot. Green dot: closest clast to the transect interval that meets the selection criteria. B. Annotated photograph showing an idealized placement of ‘windows’ (dashed black squares) on a bedrock outcrop. Outcrop dimensions are measured and the windows are placed using predetermined selection criteria. In this example, the windows are equally spaced along the centerline of the long-dimension of the upward-facing side of the outcrop.

Fig. 2. A. Example of the measurement of a surface exposure length (L; yellow line) of a fracture meeting the criteria in Table 1. The ‘h’ refers to the location where sheet height would be measured for this surface parallel fracture. B. Example of fractures that may appear to be a single fracture (left), but upon close examination are in fact multiple fractures intersecting and/or separated by rock (right inset). Arrow points to the location of the inset image on the main image. Compass in the foreground for scale.

Fig. 3. Example histograms and statistics of fracture length data measured on the exposed surfaces of clasts 15-50 cm max diameter. Upper row are data for clasts found on a modern ephemeral stream boulder bar. Clasts overall have very low fracture number density. Lower row are data for clasts on an ~6 ka surface where fracture number density is much higher. Note that it takes about 100 clasts to arrive at a statistically significant power law distribution for the Modern Wash clasts, but only 5 rocks for the rocks with higher fracture densities. Producing histograms interactively as data is collected can help establish how many observation areas are necessary for a given site.

Fig. 4. Reduced size image of an 8.5” x 11” ‘fracture sheet’ to be employed in the field to increase efficiency and to reduce ‘missing’ data. Sheet templates for both clasts and outcrops that can be modified are provided in Data Supplement as well as a data-entry template.

Fig. 5. Visual aide for estimating the abundance of “countable” rock features – including fractures. An index of 0-4 is assigned depending on the abundance of features within an average of any given observation area (ex: 10 x 10 cm) on the clast or window being examined. The area of observation is defined by the size of the features being measured. A 10 cm x 10 cm square is used for estimating the abundance of ‘fractures < 2 cm’ defined as fractures with lengths of >0.5 cm but < 2 cm (see section 5.2 for details of how to use the index). For features ≤ 0.5 cm, a 1 cm x 1 cm area would be employed and for features ≥ 2 cm, a 1 x 1 m area.

Fig. 6. A visual percent estimator (modified from Terry and Chilingar, 1955). Estimator should be employed in every estimate of percentages. See section 5.2 for using the estimator to assign a percent coverage index to features that are not countable or vary in size (e.g., lichen coverage, fine mafic minerals, etc.).

Fig. 7. **Inset:** Roundness and sphericity chart – modified from Krumbein and Sloss (1951). **Roundness:** A = angular; SA = subangular; SR = subrounded; R = rounded; WR = well-rounded. **Sphericity:** S = spherical; SS = subspherical; SE = sub-elongate; E = elongate. **Edges:** fracture comparator whereby the width most closely matching the fracture aperture is noted. Note: a to-scale pdf is available in the Data Supplement, however, owing to printing and publication scaling, it is highly recommended to calibrate the comparator prior to using it in the field.

Fig. 8 Depiction of types of fracture intersection nodes. I-nodes comprise fracture terminations with no connections. Y-nodes are abutting fractures that do not cross. X-nodes are fractures that cross. C-nodes are ‘contingent nodes’ defined by the user. In this example the rule is related to the distance between I-nodes. For #1, the distance is wider than the criteria, so the terminations are designated as I-nodes. For #2, the distance is within the limits, and the ‘connection’ is designated as a C-node.

Fig. 9. Examples of aperture transects that are appropriate for measurement of fracture aperture widths (green) and transects where there is evidence that the fracture walls have been eroded or chipped and therefore should not be employed for a width

993 measurement (red). In cases where it is not clear if erosion or chipping has occurred (orange), a note can be made for the fracture
994 width to possibly eliminate outliers during data analysis.

995

996

997 Fig. 10. Box and whisker plots of case example data collected by five different pairs of workers on the same geomorphic surface.

998 "x"s mark the means. Groups 1-4 were novice workers. Group 5 comprised one experienced worker. A. Fracture lengths B.

999 Fractures per rock C. Clast length

1000

1001

1002 *Table 1. List of proposed rule-based criteria for defining measurable fractures*

<p>The answer to the following questions must be ‘yes’ for all measured fractures. Measure all fractures meeting these criteria within the observation area.</p>	<p><u>NOTES</u></p>
<ul style="list-style-type: none"> • Is the feature a lineament longer than it is wide? • Does the lineament contain open space bounded by walls? • If the lineament is not open, can the infilling material (ex: dust and lichens) be readily scraped out? • If the lineament is open or after the material has been scraped out, is the opening deeper than it is wide <u>and</u> bounded by ~parallel walls? • Is the open portion of the lineament ≥ 2 cm (>10 grains) in length (without interrupting bridges of rock or cemented infilling material)? 	<p>Do not measure:</p> <ul style="list-style-type: none"> • Spherical pores/vesicles. • Lineaments, or portions of lineaments, with solid mineral infilling/cement. • Ledge edges or linear etchings. • rock bridges between fractures

1003

1004 *Table 2. List of proposed data to collect for the rock observation area and for all fractures ≥ 2 cm in length*

<p>Rock Observations</p>	<p>Individual Fracture Observations</p>
<ul style="list-style-type: none"> • Dimensions of the observation area (e.g. clast, outcrop, and/or window length, width, height) • Rock type • Grain size • Mineralogy % (minimally felsic vs. mafic) • Sphericity of exposure • Roundness of exposure • Fabric description, strike, and dip (e.g. vein, foliation, bedding) • Granular Disintegration • Pitting • Lichen and Varnish • Fracture Connectivity • Fracture Spacing 	<ul style="list-style-type: none"> • Length (surface exposure length measured with a flexible tape) • Aperture width: center and maximum widths measured with calipers and/or comparator • Strike 0-360° (right-hand rule preferred) • Dip 0-90° • Parallelism (note features parallel to the fracture such as fabric, rock faces) • Sheet height (the thickness of what would be the detached spall or sheet of rock above a surface parallel fracture) • Weathering Index

1005

1006

1007

1008 *Table 3. List of field equipment*

<p>Required</p>	<p>Recommended</p>
<ul style="list-style-type: none"> • Hand lens (large, 10x) • Grain size card • Fracture comparator (for fracture widths) • Flexible seamstress tape measure (with mm) • Calipers (mm 0.0 to 150) • Brunton or similar compass • Roundness and sphericity chart • Visual percentage estimator • Fracture sheets 	<ul style="list-style-type: none"> • Camera with macro lens • Chalk for marking measured fractures and windows • Safety pin or needle for fracture exploration • Cardboard cutout frames for windows • Small white board or chalk board for including observation area ID in photos

1009

1010

1011 Bibliography

- 1012** Aich, S. and Gross, M. R.: Geospatial analysis of the association between bedrock fractures and vegetation in an arid environment, **1013** *International Journal of Remote Sensing*, 29, 6937-6955, [10.1080/01431160802220185](https://doi.org/10.1080/01431160802220185), 2008.
- 1014** Al-Fahmi, M. M., Hooker, J. N., Al-Mojel, A. S., and Cartwright, J. A.: New scaling of fractures in a giant carbonate platform **1015** from outcrops and subsurface, *Journal of Structural Geology*, 140, 104142, <https://doi.org/10.1016/j.jsg.2020.104142>, 2020.
- 1016** Aldred, J., Eppes, M. C., Aquino, K., Deal, R., Garbini, J., Swami, S., Tuttle, A., and Xanthos, G.: The influence of solar-induced **1017** thermal stresses on the mechanical weathering of rocks in humid mid-latitudes, *Earth Surface Processes and Landforms*, 41, 603- **1018** 614, 2015.
- 1019** Alneasan, M. and Behnia, M.: An experimental investigation on tensile fracturing of brittle rocks by considering the effect of grain **1020** size and mineralogical composition, *International Journal of Rock Mechanics and Mining Sciences*, 137, 104570, **1021** <https://doi.org/10.1016/j.ijrmmms.2020.104570>, 2021.
- 1022** Anderson, T. L.: *Fracture Mechanics: Fundamentals and Applications*, Third, Taylor & Francis Group, Boca Raton, FL, 2005.
- 1023** Andresen, C. A., Hansen, A., Le Goc, R., Davy, P., and Hope, S. M.: Topology of fracture networks, *Frontiers in physics*, 1, 7, **1024** [10.3389/fphy.2013.00007](https://doi.org/10.3389/fphy.2013.00007), 2013.
- 1025** Andrews, B. J., Roberts, J. J., Shipton, Z. K., Bigi, S., Tartarello, M. C., and Johnson, G.: How do we see fractures? Quantifying **1026** subjective bias in fracture data collection, *Solid Earth*, 10, 487, 2019.
- 1027** ASTM: D7012-14: Standard Test Methods for Compressive Strength and Elastic Moduli of Intact Rock Core Specimens Under **1028** Varying States of Stress and Temperatures, 2017.
- 1029** Atkinson, B. K.: *Fracture Mechanics of Rock*, Academic Press Geology Series, Academic Press Inc., Orlando, Florida, **1030** <https://doi.org/10.1016/C2009-0-21691-6>, 1987.
- 1031** Ayatollahi, M. R. and Akbardoost, J.: Size and geometry effects on rock fracture toughness: Mode I fracture, *Rock Mechanics and **1032*** *Rock Engineering*, 47, 677-687, [10.1007/s00603-013-0430-7](https://doi.org/10.1007/s00603-013-0430-7), 2014.
- 1033** Aydin, A. and Basu, A.: The Schmidt hammer in rock material characterization, *Engineering Geology*, 81, 1-14, **1034** <https://doi.org/10.1016/j.enggeo.2005.06.006>, 2005.
- 1035** Baecher, G. B.: Statistical analysis of rock mass fracturing, *Journal of the International Association for Mathematical Geology*, 15, **1036** 329-348, [10.1007/BF01036074](https://doi.org/10.1007/BF01036074), 1983.
- 1037** Balco, G.: Technical note: A prototype transparent-middle-layer data management and analysis infrastructure for cosmogenic- **1038** nuclide exposure dating, *Geochronology*, 2, 169-175, <https://doi.org/10.5194/gchron-2-169-2020>, 2020.
- 1039** Barthélémy, J.-F., Guiton, M. L. E., and Daniel, J.-M.: Estimates of fracture density and uncertainties from well data, *International **1040*** *Journal of Rock Mechanics and Mining Sciences*, 46, 590-603, <https://doi.org/10.1016/j.ijrmmms.2008.08.003>, 2009.
- 1041** Barton, C. C. and Hsieh, P. A.: *Physical and Hydrologic-Flow Properties of Fractures: Las Vegas, Nevada - Zion Canyon, Utah - **1042*** *Grand Canyon, Arizona - Yucca Mountain, Nevada, July 20-24, 1989 (Field Trip Guidebook T385)*, American Geophysical Union, **1043** Washington, D.C.1989.
- 1044** Barton, C. C., Larsen, E., Page, W. R., and Howard, T. M.: Characterizing fractured rock for fluid-flow, geomechanical, and **1045** paleostress modeling: Methods and preliminary results from Yucca Mountain, Nevada, United States, Medium: ED; Size: 74 p., **1046** [10.2172/145208](https://doi.org/10.2172/145208), 1993.
- 1047** Berberich, S.: *A chronosequence of cracking in Mill Creek, California*, Geography and Earth Sciences, The University of North **1048** Carolina Charlotte, ProQuest, 2020.
- 1049** Berkowitz, B.: Characterizing flow and transport in fractured geological media: A review, *Advances in Water Resources*, 25, 861- **1050** 884, [https://doi.org/10.1016/S0309-1708\(02\)00042-8](https://doi.org/10.1016/S0309-1708(02)00042-8), 2002.
- 1051** Birkeland, P. W.: *Soils and Geomorphology*, Oxford University Press, New York, New York, 1999.
- 1052** Bonnet, E., Bour, O., Odling, N. E., Davy, P., Main, I., Cowie, P., and Berkowitz, B.: Scaling of fracture systems in geological **1053** media, *Reviews of Geophysics*, 39, 347-383, 2001.
- 1054** Borg, I. and Handin, J.: Experimental deformation of crystalline rocks, *Tectonophysics*, 3, 249-367, [1951\(66\)90019-9](https://doi.org/10.1016/0040- 1055 <a href=), 1966.

- 1056** Brantley, S. L., Eissenstat, D. M., Marshall, J. A., Godsey, S. E., Balogh-Brunstad, Z., Karwan, D. L., Papuga, S. A., Roering, J.,
1057 Dawson, T. E., Evaristo, J., Chadwick, O., McDonnell, J. J., and Weathers, K. C.: Reviews and syntheses: On the roles trees play
1058 in building and plumbing the critical zone, *Biogeosciences*, 14, 5115, 2017.
- 1059** Brantut, N., Heap, M. J., Meredith, P. G., and Baud, P.: Time-dependent cracking and brittle creep in crustal rocks: A review,
1060 *Journal of Structural Geology*, 52, 17-43, 2013.
- 1061** Brilha, J., Gray, M., Pereira, D. I., and Pereira, P.: Geodiversity: An integrative review as a contribution to the sustainable
1062 management of the whole of nature, *Environmental Science & Policy*, 86, 19-28, <https://doi.org/10.1016/j.envsci.2018.05.001>,
1063 2018.
- 1064** Buckman, S., Morris, R. H., and Bourman, R. P.: Fire-induced rock spalling as a mechanism of weathering responsible for flared
1065 slope and inselberg development, *Nature Communications*, 12, 2150, [10.1038/s41467-021-22451-2](https://doi.org/10.1038/s41467-021-22451-2), 2021.
- 1066** Burghelca, C., Zaharescu, D. G., Dontsova, K., Maier, R., Huxman, T., and Chorover, J.: Mineral nutrient mobilization by plants
1067 from rock: influence of rock type and arbuscular mycorrhiza, *Biogeochemistry*, 124, 187-203, [10.1007/s10533-015-0092-5](https://doi.org/10.1007/s10533-015-0092-5), 2015.
- 1068** Burke, R. M. and Birkeland, P. W.: Reevaluation of multiparameter relative dating techniques and their application to the glacial
1069 sequence along the eastern escarpment of the Sierra Nevada, California, *Quaternary Research*, 11, 21-51, [10.1016/0033-5894\(79\)90068-1](https://doi.org/10.1016/0033-5894(79)90068-1), 1979.
- 1071** Burnett, B. N., Meyer, G. A., and McFadden, L. D.: Aspect-related microclimatic influences on slope forms and processes,
1072 northeastern Arizona, *Journal of Geophysical Research: Earth Surface*, 113, <https://doi.org/10.1029/2007JF000789>, 2008.
- 1073** Buss, H. L., Sak, P. B., Webb, S. M., and Brantley, S. L.: Weathering of the Rio Blanco quartz diorite, Luquillo Mountains, Puerto
1074 Rico: Coupling oxidation, dissolution, and fracturing, *Geochimica et Cosmochimica Acta*, 72, 4488-4507, 2008.
- 1075** Chen, X., Eichhubl, P., and Olson, J. E.: Effect of water on critical and subcritical fracture properties of Woodford shale, *Journal*
1076 *of Geophysical Research: Solid Earth*, 122, 2736-2750, <https://doi.org/10.1002/2016JB013708>, 2017.
- 1077** Chilton, K. D. and Spotila, J. A.: Preservation of Valley and Ridge topography via delivery of resistant, ridge-sourced boulders to
1078 hillslopes and channels, Southern Appalachian Mountains, U.S.A., *Geomorphology*, 365, 107263,
1079 <https://doi.org/10.1016/j.geomorph.2020.107263>, 2020.
- 1080** Clauset, A., Shalizi, C. R., and Newman, M. E. J.: Power-law distributions in empirical data, *SIAM review*, 51, 661-703,
1081 [10.1137/070710111](https://doi.org/10.1137/070710111), 2009.
- 1082** Collins, B. D. and Stock, G. M.: Rockfall triggering by cyclic thermal stressing of exfoliation fractures, *Nature Geoscience*, 9, 395-
1083 401, 2016.
- 1084** Coombes, M. A., Viles, H. A., and Zhang, H.: Thermal blanketing by ivy (*Hedera helix* L.) can protect building stone from
1085 damaging frosts, *Nature: Scientific Reports*, 8, 1-12, 2018.
- 1086** Corrêa, R. S. M., Marrett, R., and Laubach, S. E.: Analysis of spatial arrangement of fractures in two dimensions using point
1087 process statistics, *Journal of Structural Geology*, 163, 104726, <https://doi.org/10.1016/j.jsg.2022.104726>, 2022.
- 1088** Cox, R., Lopes, W. A., and Jahn, K. L.: Quantitative roundness analysis of coastal boulder deposits, *Marine Geology*, 396, 114-
1089 141, <https://doi.org/10.1016/j.margeo.2017.03.003>, 2018.
- 1090** Cuccuru, S., Casini, L., Oggiano, G., and Cherchi, G. P.: Can weathering improve the toughness of a fractured rock? A case study
1091 using the San Giacomo granite, *Bulletin of Engineering Geology Environments*, 71, 557-567, 2012.
- 1092** Davy, P., Le Goc, R., Darcel, C., Bour, O., de Dreuzy, J. R., and Munier, R.: A likely universal model of fracture scaling and its
1093 consequence for crustal hydromechanics, *Journal of Geophysical Research: Solid Earth*, 115,
1094 <https://doi.org/10.1029/2009JB007043>, 2010.
- 1095** Dershowitz, W. S. and Herda, H. H.: Interpretation of fracture spacing and intensity, *The 33rd U.S. Symposium on Rock Mechanics*
1096 (USRMS), 1992.
- 1097** DiBiase, R. A., Rossi, M. W., and Neely, A. B.: Fracture density and grain size controls on the relief structure of bedrock
1098 landscapes, *Geology*, 48, 399-402, 2018.
- 1099** Domokos, G., Jerolmack, D. J., Kun, F., and Torok, J.: Plato's cube and the natural geometry of fragmentation, *Proceedings of the*
1100 *National Academy of Sciences*, 117, 18178-18185, 2020.
- 1101** Dove, P. M.: Geochemical controls on the kinetics of quartz fracture at subcritical tensile stresses, *Journal of Geophysical Research*,
1102 100, 349-359, 1995.

- 1103** Engelder, T.: *Stress Regimes in the Lithosphere*, Princeton University Press, 1993.
- 1104** English, J. M. and Laubach, S. E.: Opening-mode fracture systems: insights from recent fluid inclusion microthermometry studies of crack-seal fracture cements, *Geological Society, London, Special Publications*, 458, 257-272, doi:10.1144/SP458.1, 2017.
- 1105**
- 1106** Eppes, M.-C., 2022. Mechanical Weathering: A Conceptual Overview. In: Shroder, J.J.F. (Ed.), *Treatise on Geomorphology*, vol. 3. Elsevier, Academic Press, pp. 30–45. <https://dx.doi.org/10.1016/B978-0-12-818234-5.00200-5>.
- 1107**
- 1108** Eppes, M. C. and Griffing, D.: Granular disintegration of marble in nature: A thermal-mechanical origin for a grus and corestone landscape, *Geomorphology*, 117, 170-180, 2010.
- 1109**
- 1110** Eppes, M. C. and Keanini, R.: Mechanical weathering and rock erosion by climate-dependent subcritical cracking, *Reviews of Geophysics*, 55, 470-508, 2017.
- 1111**
- 1112** Eppes, M. C., McFadden, L. D., Wegmann, K. W., and Scuderi, L. A.: Cracks in desert pavement rocks: Further insights into mechanical weathering by directional insolation, *Geomorphology*, 123, 97-108, 2010.
- 1113**
- 1114** Eppes, M. C., Magi, B., Scheff, J., Warren, K., Ching, S., and Feng, T.: Warmer, wetter climates accelerate mechanical weathering in field data, independent of stress-loading, *Geophysical Research Letters*, 47, 1-11, 2020.
- 1115**
- 1116** Eppes, M. C., Magi, B., Hallet, B., Delmelle, E., Mackenzie-Helnwein, P., Warren, K., and Swami, S.: Deciphering the role of solar-induced thermal stresses in rock weathering, *GSA Bulletin*, 128, 1315-1338, 2016.
- 1117**
- 1118** Eppes, M. C., Hancock, G. S., Chen, X., Arey, J., Dewers, T., Huettenmoser, J., Kiessling, S., Moser, F., Tannu, N., Weiserbs, B., and Whitten, J.: Rates of subcritical cracking and long-term rock erosion, *Geology*, 46, 951-954, 2018.
- 1119**
- 1120** Fisher, N. I.: *Statistical Analysis of Circular Data*, Cambridge University Press, Cambridge, England, <https://doi.org/10.1017/CBO9780511564345>, 1993.
- 1121**
- 1122** Forstner, S. R. and Laubach, S. E.: Scale-dependent fracture networks, *Journal of Structural Geology*, 165, 104748, <https://doi.org/10.1016/j.jsg.2022.104748>, 2022.
- 1123**
- 1124** Girard, L., Gruber, S., Weber, S., and Beutel, J.: Environmental controls of frost cracking revealed through in situ acoustic emission measurements in steep bedrock, *Geophysical Research Letters*, 40, 1748-1753, 10.1002/grl.50384, 2013.
- 1125**
- 1126** Gischig, V. S., Moore, J. R., Evans, K. F., Amann, F., and Loew, S.: Thermomechanical forcing of deep rock slope deformation: I. Conceptual study of a simplified slope, *Journal of Geophysical Research*, 116, 10.1029/2011JF002006, 2011.
- 1127**
- 1128** Glade, R. C., Shobe, C. M., Anderson, R. S., and Tucker, G. E.: Canyon shape and erosion dynamics governed by channel-hillslope feedbacks, *Geology*, 47, 650-654, 10.1130/G46219.1, 2019.
- 1129**
- 1130** Gomez-Heras, M., Smith, B. J., and Fort, R.: Surface temperature differences between minerals in crystalline rocks: Implications for granular disaggregation of granites through thermal fatigue, *Geomorphology*, 78, 236-249, 2006.
- 1131**
- 1132** Gómez-Pujol, L., Fornós, J. J., and Swantesson, J. O. H.: Rock surface millimetre-scale roughness and weathering of supratidal Mallorcan carbonate coasts (Balearic Islands), *Earth Surface Processes and Landforms*, 31, 1792-1801, <https://doi.org/10.1002/esp.1379>, 2006.
- 1133**
- 1134**
- 1135** Griffiths, L., Heap, M. J., Baud, P., and Schmittbuhl, J.: Quantification of microcrack characteristics and implications for stiffness and strength of granite, *International Journal of Rock Mechanics and Mining Sciences*, 100, 138-150, <https://doi.org/10.1016/j.ijrmms.2017.10.013>, 2017.
- 1136**
- 1137**
- 1138** Hancock, G. S. and Kirwan, M.: Summit erosion rates deduced from ¹⁰Be: Implications for relief production in the central Appalachians, *Geology*, 35, 89-92, 10.1130/g23147a.1, 2007.
- 1139**
- 1140** Hancock, P. L.: Brittle microtectonics: Principles and practice, *Journal of Structural Geology*, 7, 437-457, [https://doi.org/10.1016/0191-8141\(85\)90048-3](https://doi.org/10.1016/0191-8141(85)90048-3), 1985.
- 1141**
- 1142** Handin, J. and Hager, R. V., Jr.: Experimental deformation of sedimentary rocks under confining pressure: Tests at room temperature on dry samples, *AAPG Bulletin*, 41, 1-50, 10.1306/5ceae5fb-16bb-11d7-8645000102c1865d, 1957.
- 1143**
- 1144** Handin, J. and Hager, R. V., Jr.: Experimental deformation of sedimentary rocks under confining pressure: Tests at high temperature, *AAPG Bulletin*, 42, 2892-2934, 10.1306/0bda5c27-16bd-11d7-8645000102c1865d, 1958.
- 1145**
- 1146** Handin, J., Hager Jr, R. V., Friedman, M., and Feather, J. N.: Experimental deformation of sedimentary rocks under confining pressure: Pore pressure tests, *AAPG Bulletin*, 47, 717-755, 1963.
- 1147**

- 1148** Hasenmueller, E. A., Gu, X., Weitzman, J. N., Adams, T. S., Stinchcomb, G. E., Eissenstat, D. M., Drohan, P. J., Brantley, S. L.,
1149 and Kaye, J. P.: Weathering of rock to regolith: The activity of deep roots in bedrock fractures, *Geoderma*, 300, 11-31,
1150 <https://doi.org/10.1016/j.geoderma.2017.03.020>, 2017.
- 1151** Hatir, M. E.: Determining the weathering classification of stone cultural heritage via the analytic hierarchy process and fuzzy
1152 inference system, *Journal of Cultural Heritage*, 44, 120-134, <https://doi.org/10.1016/j.culher.2020.02.011>, 2020.
- 1153** He, M., Xia, H., Jia, X., Gong, W., Zhao, F., and Liang, K.: Studies on classification, criteria, and control of rockbursts, *Journal of*
1154 *Rock Mechanics and Geotechnical Engineering*, 4, 97-114, 10.3724/SP.J.1235.2012.00097, 2012.
- 1155** Healy, D., Rizzo, R. E., Cornwell, D. G., Farrell, N. J. C., Watkins, H., Timms, N. E., Gomez-Rivas, E., and Smith, M.: FracPaQ:
1156 A MATLAB™ toolbox for the quantification of fracture patterns, *Journal of Structural Geology*, 95, 1-16,
1157 <https://doi.org/10.1016/j.jsg.2016.12.003>, 2017.
- 1158** Heard, H. C.: Effect of large changes in strain rate in the experimental deformation of Yule Marble, *The Journal of Geology*, 71,
1159 162-195, 1963.
- 1160** Heidbach, O., Rajabi, M., Cui, X., Fuchs, K., Müller, B., Reinecker, J., Reiter, K., Tingay, M., Wenzel, F., Xie, F., Ziegler, M. O.,
1161 Zoback, M.-L., and Zoback, M.: The World Stress Map database release 2016: Crustal stress pattern across scales, *Tectonophysics*,
1162 744, 484-498, <https://doi.org/10.1016/j.tecto.2018.07.007>, 2018.
- 1163** Holder, J., Olson, J. E., and Philip, Z.: Experimental determination of subcritical crack growth parameters in sedimentary rock,
1164 *Geophysical Research Letters*, 28, 599-602, <https://doi.org/10.1029/2000GL011918>, 2001.
- 1165** Hooke, R.: Geomorphic evidence for Late-Wisconsin and Holocene tectonic deformation, Death Valley, California, *GSA Bulletin*,
1166 83, 2073-2098, 10.1130/0016-7606(1972)83[2073:Geflah]2.0.Co;2, 1972.
- 1167** Hooker, J. N., Laubach, S. E., and Marrett, R.: A universal power-law scaling exponent for fracture apertures in sandstones, *GSA*
1168 *Bulletin*, 126, 1340-1362, 10.1130/b30945.1, 2014.
- 1169** Hooker, J. N., Gale, J. F. W., Gomez, L. A., Laubach, S. E., Marrett, R., and Reed, R. M.: Aperture-size scaling variations in a
1170 low-strain opening-mode fracture set, Cozzette Sandstone, Colorado, *Journal of Structural Geology*, 31, 707-718,
1171 <https://doi.org/10.1016/j.jsg.2009.04.001>, 2009.
- 1172** Isherwood, D. and Street, A.: Biotite-induced grossification of the Boulder Creek Granodiorite, Boulder County, Colorado, *GSA*
1173 *Bulletin*, 87, 366-370, 10.1130/0016-7606(1976)87<366:Bgotbc>2.0.Co;2, 1976.
- 1174** Janio de Castro Lima, J. and Paraguassú, A. B.: Linear thermal expansion of granitic rocks: influence of apparent porosity, grain
1175 size and quartz content, *Bulletin of Engineering Geology and the Environment*, 63, 215-220, 10.1007/s10064-004-0233-x, 2004.
- 1176** Jenny, H.: *Factors of Soil Formation: A System of Quantitative Pedology*, McGraw-Hill, New York, New York, 1941.
- 1177** Kobayashi, A. S. and Enetanya, A. N.: Stress intensity factor of a corner crack, *Mechanics of Crack Growth*, 1976.
- 1178** Kranz, R. L.: Microcrack in rocks: A review, *Tectonophysics*, 100, 449-480, 1983.
- 1179** Krumbein, W. C.: Fundamental attributes of sedimentary particles, *University of Iowa Student Engineering Bulletin*, 27, 318-331,
1180 1943.
- 1181** Krumbein, W. C. and Sloss, L. L.: *Stratigraphy and Sedimentation*, W. H. Freeman and Company, San Francisco, California, 1951.
- 1182** Lamp, J. L., Marchant, D. R., Mackay, S. L., and Head, J. W.: Thermal stress weathering and the spalling of Antarctic rocks,
1183 *Journal of Geophysical Research: Earth Surface*, 122, 3-24, <https://doi.org/10.1002/2016JF003992>, 2017.
- 1184** Laubach, S. E., Olson, J. E., and Gross, M. R.: Mechanical and fracture stratigraphy, *AAPG Bulletin*, 93, 1413-1426,
1185 10.1306/07270909094, 2009.
- 1186** Laubach, S. E., Lamarche, J., Gauthier, B. D. M., Dunne, W. M., and Sanderson, D. J.: Spatial arrangement of faults and opening-
1187 mode fractures, *Journal of Structural Geology*, 108, 2-15, <https://doi.org/10.1016/j.jsg.2017.08.008>, 2018.
- 1188** Laubach, S. E., Lander, R. H., Criscenti, L. J., Anovitz, L. M., Urai, J. L., Pollyea, R. M., Hooker, J. N., Narr, W., Evans, M. A.,
1189 Kerisit, S. N., Olson, J. E., Dewers, T., Fisher, D., Bodnar, R., Evans, B., Dove, P., Bonnell, L. M., Marder, M. P., and Pyrak-
1190 Nolte, L.: The role of chemistry in fracture pattern development and opportunities to advance interpretations of geological
1191 materials, *Reviews of Geophysics*, 57, 1065-1111, 10.1029/2019RG000671, 2019.
- 1192** Leith, K., Moore, J. R., Amann, F., and Loew, S.: In situ stress control on microcrack generation and macroscopic extensional
1193 fracture in exhuming bedrock, *Journal of Geophysical Research*, 119, 1-22, 2014.

- 1194** Leone, J. D., Holbrook, W. S., Reibe, C. S., Chorover, J., Ferre, T. P. A., Carr, B. J., and Callahan, R. P.: Strong slope-aspect control of regolith thickness by bedrock foliation, *Earth Surface Processes and Landforms*, 45, 2998-3010, 2020.
- 1196** Long, J., Jones, R., Daniels, S., Gilment, S., Oxlade, D., and Wilkinson, M.: Reducing uncertainty in fracture modelling: Assessing user bias in interpretations from satellite imagery, AAPG 2019 Annual Convention & Exhibition, San Antonio, TX, 2019.
- 1198** Long, J. C. S. and Witherspoon, P. A.: The relationship of the degree of interconnection to permeability in fracture networks, *Journal of Geophysical Research: Solid Earth*, 90, 3087-3098, <https://doi.org/10.1029/JB090iB04p03087>, 1985.
- 1200** Macholdt, D. S., Al-Amri, A. M., Tuffaha, H. T., Jochum, K. P., and Andreae, M. O.: Growth of desert varnish on petroglyphs from Jubbah and Shuwaymis, Ha'il region, Saudi Arabia, *The Holocene*, 28, 1495-1511, [10.1177/0959683618777075](https://doi.org/10.1177/0959683618777075), 2018.
- 1202** Maffucci, R., Bigi, S., Corrado, S., Chiodi, A., Di Paolo, L., Giordano, G., and Invernizzi, C.: Quality assessment of reservoirs by means of outcrop data and "discrete fracture network" models: The case history of Rosario de La Frontera (NW Argentina) geothermal system, *Tectonophysics*, 647-648, 112-131, <https://doi.org/10.1016/j.tecto.2015.02.016>, 2015.
- 1205** Manzocchi, T.: The connectivity of two-dimensional networks of spatially correlated fractures, *Water Resources Research*, 38, 1-1-20, <https://doi.org/10.1029/2000WR000180>, 2002.
- 1207** Mardia, K. V. and Jupp, P. E.: *Directional Statistics*, Academic Press Inc., London, England, 1972.
- 1208** Marrett, R., Gale, J. F. W., Gómez, L. A., and Laubach, S. E.: Correlation analysis of fracture arrangement in space, *Journal of Structural Geology*, 108, 16-33, <https://doi.org/10.1016/j.jsg.2017.06.012>, 2018.
- 1210** Marshall, J., Clyne, J., Eppes, M. C., and Dawson, T.: Barking up the wrong tree? Tree root tapping, subcritical cracking, and potential influence on bedrock porosity, AGU 2021 Fall Abstracts, 2021a.
- 1212** Marshall, J. A., Roering, J. J., Rempel, A. W., Shafer, S. L., and Bartlein, P. J.: Extensive frost weathering across unglaciated North America during the Last Glacial Maximum, *Geophysical Research Letters*, 48, <https://doi.org/10.1029/2020GL090305>, 2021b.
- 1215** Martel, S. J.: Effect of topographic curvature on near-surface stresses and application to sheeting joints, *Geophysical Research Letters*, 33, 2006.
- 1217** Martel, S. J.: Mechanics of curved surfaces, with application to surface-parallel cracks, *Geophysical Research Letters*, 38, 2011.
- 1218** Martel, S. J.: Progress in understanding sheeting joints over the past two centuries, *Journal of Structural Geology*, 94, 68-86, 2017.
- 1219** Matsuoka, N. and Murton, J.: Frost weathering: Recent advances and future directions, *Permafrost and Periglacial Processes*, 19, 195-210, [10.1002/ppp.620](https://doi.org/10.1002/ppp.620), 2008.
- 1221** Matthews, J. A. and Winkler, S.: Schmidt-hammer exposure-age dating: A review of principles and practice, *Earth-Science Reviews*, 230, 104038, <https://doi.org/10.1016/j.earscirev.2022.104038>, 2022.
- 1223** McAuliffe, J. R., McFadden, L. D., Persico, L. P., and Rittenour, T. M.: Climate and vegetation change, hillslope soil erosion, and the complex nature of Late Quaternary environmental transitions, Eastern Mojave Desert, USA, *Quaternary*, 5, 43, 2022.
- 1225** McCarroll, D.: The Schmidt hammer, weathering, and rock surface roughness, *Earth Surface Processes and Landforms*, 16, 477-480, <https://doi.org/10.1002/esp.3290160510>, 1991.
- 1227** McFadden, L. D. and Hendricks, D. M.: Changes in the content and composition of pedogenic iron oxyhydroxides in a chronosequence of soils in southern California, *Quaternary Research*, 23, 189-204, [https://doi.org/10.1016/0033-5894\(85\)90028-6](https://doi.org/10.1016/0033-5894(85)90028-6), 1985.
- 1230** McFadden, L. D., Eppes, M. C., Gillespie, A. R., and Hallet, B.: Physical weathering in arid landscapes due to diurnal variation in the direction of solar heating, *GSA Bulletin*, 117, 161-173, 2005.
- 1232** Mogi, K.: Effect of the intermediate principal stress on rock failure, *Journal of Geophysical Research (1896-1977)*, 72, 5117-5131, <https://doi.org/10.1029/JZ072i020p05117>, 1967.
- 1234** Mogi, K.: Fracture and flow of rocks under high triaxial compression, *Journal of Geophysical Research (1896-1977)*, 76, 1255-1269, <https://doi.org/10.1029/JB076i005p01255>, 1971.
- 1236** Molaro, J. L., Byrne, S., and Le, J.-L.: Thermally induced stresses in boulders on airless body surfaces, and implications for rock breakdown, *Icarus*, 294, 247-261, 2017.

- 1238** Molaro, J. L., Hergenrother, C. W., Chesley, S. R., Walsh, K. J., Hanna, R. D., Haberle, C. W., Schwartz, S. R., Ballouz, R.-L.,
1239 Bottke, W. F., Campins, H. J., and Lauretta, D. S.: Thermal fatigue as a driving mechanism for activity on asteroid Bennu, *Journal*
1240 *of Geophysical Research*, 125, 1-24, 10.1029/2019JE006325, 2020.
- 1241** Molnar, P.: Interactions among topographically induced elastic stress, static fatigue, and valley incision, *Journal of Geophysical*
1242 *Research*, 109, 1-9, 10.1029/2003JF000097, 2004.
- 1243** Moon, S., Perron, J. T., Martel, S. J., Goodfellow, B. W., Ivars, D. M., Hall, A., Heyman, J., Munier, R., Naslund, J., Simeonov,
1244 A., and Stroeven, A. P.: Present-day stress field influences bedrock fracture openness deep into the subsurface, *Geophysical*
1245 *Research Letters*, 47, 1-10, 2020.
- 1246** Moon, S., Perron, J. T., Martel, S. J., Goodfellow, B. W., Mas Ivars, D., Simeonov, A., Munier, R., Naslund, J.-O., Hall, A.,
1247 Stroeven, A. P., Ebert, K., and Heyman, J.: Landscape features influence bedrock fracture openness in the deep subsurface,
1248 *Geological Society of American Annual Meeting*, Phoenix, AZ, USA, 10.1130/abs/2019AM-336309,
- 1249** Moser, F.: Spatial and temporal variance in rock dome exfoliation and weathering near Twain Harte, California, USA, *Geography*
1250 *and Earth Sciences*, The University of North Carolina Charlotte, ProQuest, 2017.
- 1251** Mushkin, A., Sagy, A., Trabelci, E., Amit, R., and Porat, N.: Measure the time and scale-dependency of subaerial rock weathering
1252 rates over geologic time scales with ground-based lidar, *Geology*, 42, 1063-1066, 2014.
- 1253** Nara, Y. and Kaneko, K.: Sub-critical crack growth in anisotropic rock, *International Journal of Rock Mechanics and Mining*
1254 *Sciences*, 43, 437-453, <https://doi.org/10.1016/j.ijrmms.2005.07.008>, 2006.
- 1255** Nara, Y., Kashiwaya, K., Nishida, Y., and Ii, T.: Influence of surrounding environment on subcritical crack growth in marble,
1256 *Tectonophysics*, 706-707, 116-128, 2017.
- 1257** Nara, Y., Morimoto, K., Hiroyoshi, N., Yoneda, T., Kaneko, K., and Benson, P. M.: Influence of relative humidity on fracture
1258 toughness of rock: Implications for subcritical crack growth, *International Journal of Solids and Structures*, 49, 2471-2481,
1259 <https://doi.org/10.1016/j.ijsolstr.2012.05.009>, 2012.
- 1260** Narr, W. and Lerche, I.: A method for estimating subsurface fracture density in core, *AAPG Bulletin*, 68, 637-648,
1261 10.1306/ad461354-16f7-11d7-8645000102c1865d, 1984.
- 1262** Neely, A. B., DiBiase, R. A., Corbett, L. B., Bierman, P. R., and Caffee, M. W.: Bedrock fracture density controls on hillslope
1263 erodibility in steep, rocky landscapes with patchy soil cover, southern California, USA, *Earth and Planetary Science Letters*, 522,
1264 186-197, <https://doi.org/10.1016/j.epsl.2019.06.011>, 2019.
- 1265** Ollier, C. D.: *Weathering*, 2nd, Longman, London, England, 1984.
- 1266** Olsen, T., Borella, J., and Stahl, T.: Clast transport history influences Schmidt hammer rebound values, *Earth Surface Processes*
1267 *and Landforms*, 45, 1392-1400, <https://doi.org/10.1002/esp.4809>, 2020.
- 1268** Olson, J. E.: Predicting fracture swarms - the influence of subcritical crack growth and the crack-tip process zone on joint spacing
1269 in rock, *Geological Society of London Special Publications*, 231, 73-87, 2004.
- 1270** Ortega, O. and Marrett, R.: Prediction of macrofracture properties using microfracture information, Mesaverde Group sandstones,
1271 San Juan basin, New Mexico, *Journal of Structural Geology*, 22, 571-588, [https://doi.org/10.1016/S0191-8141\(99\)00186-8](https://doi.org/10.1016/S0191-8141(99)00186-8), 2000.
- 1272** Ortega, O. J., Marrett, R. A., and Laubach, S. E.: A scale-independent approach to fracture intensity and average spacing
1273 measurement, *AAPG Bulletin*, 90, 193-208, 10.1306/08250505059, 2006.
- 1274** Paris, P. and Erdogan, F.: A critical analysis of crack propagation laws, *Journal of Basic Engineering*, 85, 528-533,
1275 10.1115/1.3656900, 1963.
- 1276** Phillips, J. D.: An evaluation of the factors determining the effectiveness of water quality buffer zones, *Journal of Hydrology*, 107,
1277 133-145, [https://doi.org/10.1016/0022-1694\(89\)90054-1](https://doi.org/10.1016/0022-1694(89)90054-1), 1989.
- 1278** Ponti, S., Pezza, M., and Guglielmin, M.: The development of Antarctic tafoni: Relations between differential weathering rates
1279 and spatial distribution of thermal events, salts concentration, and mineralogy, *Geomorphology*, 373, 2021.
- 1280** Ramcharan, A., Hengl, T., Nauman, T., Brungard, C., Waltman, S., Wills, S., and Thompson, J.: Soil property and class maps of
1281 the conterminous United States at 100-meter spatial resolution, *Soil Science Society of America Journal*, 82, 186-201,
1282 <https://doi.org/10.2136/sssaj2017.04.0122>, 2018.

- 1283** Ramulu, M., Chakraborty, A. K., and Sitharam, T. G.: Damage assessment of basaltic rock mass due to repeated blasting in a railway tunnelling project – A case study, *Tunnelling and Underground Space Technology*, 24, 208-221, <https://doi.org/10.1016/j.tust.2008.08.002>, 2009.
- 1284**
- 1285**
- 1286** Rasmussen, M., Eppes, M. C., and Berberich, S.: Untangling the impacts of climate, lithology, and time on rock cracking rates and morphology in arid and semi-arid Eastern California, AGU Fall Meeting, New Orleans, LA, 2021.
- 1287**
- 1288** Ravaji, B., Ali-Lagoa, V., Delbo, M., and Wilkerson, J. W.: Unraveling the mechanics of thermal stress weathering rate-effects, size-effects, and scaling laws., *Journal of Geophysical Research*, 121, 3304-3328, [10.1029/2019JE006019](https://doi.org/10.1029/2019JE006019), 2019.
- 1289**
- 1290** Riebe, C. S., Callahan, R. P., Granke, S. B.-M., Carr, B. J., Hayes, J. L., Schell, M. S., and Sklar, L. S.: Anisovolumetric weathering in granitic saprolite controlled by climate and erosion rate, *Geology*, 1-5, [10.1130/G48191.1](https://doi.org/10.1130/G48191.1), 2021.
- 1291**
- 1292** Rossen, W. R., Gu, Y., and Lake, L. W.: Connectivity and permeability in fracture networks obeying power-law statistics, SPE Permian Basin Oil and Gas Recovery Conference, [10.2118/59720-ms](https://doi.org/10.2118/59720-ms), 2000.
- 1293**
- 1294** Røyne, A., Jamtveit, B., Mathiesen, J., and Malthe-Sørenssen, A.: Controls on rock weathering rates by reaction-induced hierarchical fracturing, *Earth and Planetary Science Letters*, 275, 364-369, <https://doi.org/10.1016/j.epsl.2008.08.035>, 2008.
- 1295**
- 1296** Sanderson, D. J.: Field-based structural studies as analogues to sub-surface reservoirs, Geological Society, London, Special Publications, 436, 207-217, [doi:10.1144/SP436.5](https://doi.org/10.1144/SP436.5), 2016.
- 1297**
- 1298** Sanderson, D. J. and Nixon, C. W.: Topology, connectivity and percolation in fracture networks, *Journal of Structural Geology*, 115, 167-177, <https://doi.org/10.1016/j.jsg.2018.07.011>, 2018.
- 1299**
- 1300** Scarciglia, F., Saporito, N., La Russa, M. F., Le Pera, E., Macchione, M., Puntillo, D., Crisci, G. M., and Pezzino, A.: Role of lichens in weathering of granodiorite in the Sila uplands (Calabria, Southern Italy), *Sedimentary Geology*, 280, 119-134, 2012.
- 1301**
- 1302** Schoeneberger, P. J., Wysocki, D. A., and Benham, E. C.: Field Book for Describing and Sampling Soils: Version 3.0, Natural Resources Conservation Service, National Soil Survey Center, Lincoln, Nebraska 2012.
- 1303**
- 1304** Schultz, R. A.: *Geologic Fracture Mechanics*, Cambridge University Press, Cambridge, England, DOI: [10.1017/9781316996737](https://doi.org/10.1017/9781316996737), 2019.
- 1305**
- 1306** Sharifigaliuk, H., Mahmood, S. M., Ahmad, M., and Rezaee, R.: Use of outcrop as substitute for subsurface shale: Current understanding of similarities, discrepancies, and associated challenges, *Energy & Fuels*, 35, 9151-9164, [10.1021/acs.energyfuels.1c00598](https://doi.org/10.1021/acs.energyfuels.1c00598), 2021.
- 1307**
- 1308**
- 1309** Shi, J.: Study of thermal stresses in rocks due to diurnal solar exposure, *Civil Engineering*, University of Washington, 58 pp., 2011.
- 1310** Shobe, C. M., Hancock, G. S., Eppes, M. C., and Small, E. E.: Field evidence for the influence of weathering on rock erodibility and channel form in bedrock rivers, *Earth Surface Processes and Landforms*, 42, 1997-2012, 2017.
- 1311**
- 1312** Sklar, L. S., Riebe, C. S., Marshall, J. A., Genetti, J., Leclere, S., Lukens, C. L., and Merces, V.: The problem of predicting the size distribution of sediment supplied by hillslopes to rivers, *Geomorphology*, 277, 31-49, 2017.
- 1313**
- 1314** Snowdon, A. P., Normani, S. D., and Sykes, J. F.: Analysis of crystalline rock permeability versus depth in a Canadian Precambrian rock setting, *Journal of Geophysical Research: Solid Earth*, 126, e2020JB020998, <https://doi.org/10.1029/2020JB020998>, 2021.
- 1315**
- 1316** Sousa, L. M. O.: Evaluation of joints in granitic outcrops for dimension stone exploitation, *Quarterly Journal of Engineering Geology and Hydrogeology*, 43, 85-94, [10.1144/1470-9236/08-076](https://doi.org/10.1144/1470-9236/08-076), 2010.
- 1317**
- 1318** St. Clair, J., Moon, S., Holbrook, W. S., Perron, J. T., Riebe, C. S., Martel, S. J., Carr, B., Harman, C., Singha, K., and Richter, D. D.: Geophysical imaging reveals topographic stress control of bedrock weathering, *Geomorphology*, 350, 534-538, 2015.
- 1319**
- 1320** Staff, Soil Survey: *Soil Taxonomy: A basic system of soil classification for making and interpreting soil surveys*, 1999.
- 1321** Terry, R. D. and Chilingar, G. V.: Summary of "Concerning some additional aids in studying sedimentary formations," by M. S. Shvetsov, *Journal of Sedimentary Research*, 25, 229-234, [10.1306/74d70466-2b21-11d7-8648000102c1865d](https://doi.org/10.1306/74d70466-2b21-11d7-8648000102c1865d), 1955.
- 1322**
- 1323** Turner, F. J., Griggs, D. T., and Heard, H. C.: Experimental deformation of calcite crystals, *GSA Bulletin*, 65, 883-934, [10.1130/0016-7606\(1954\)65\[883:Edocc\]2.0.Co;2](https://doi.org/10.1130/0016-7606(1954)65[883:Edocc]2.0.Co;2), 1954.
- 1324**
- 1325** Ukar, E., Laubach, S. E., and Hooker, J. N.: Outcrops as guides to subsurface natural fractures: Example from the Nikanassin Formation tight-gas sandstone, Grande Cache, Alberta foothills, Canada, *Marine and Petroleum Geology*, 103, 255-275, <https://doi.org/10.1016/j.marpetgeo.2019.01.039>, 2019.
- 1326**
- 1327**

- 1328** Ulusay, R. and Hudson, J. A.: The Complete ISRM Suggested Methods for Rock Characterization, Testing and Monitoring: 1974-
1329 2006, Commission on Testing Methods, International Society of Rock Mechanics., Ankara, Turkey 2007.
- 1330** Ulusay, R. e.: The ISRM Suggested Methods for Rock Characterization, Testing and Monitoring, 1, Springer International
1331 Publishing, Switzerland, 293 pp., <https://doi.org/10.1007/978-3-319-07713-0>, 2015.
- 1332** Vazquez, P., Shushakova, V., and Gomez-Heras, M.: Influence of mineralogy on granite decay induced by temperature increase:
1333 Experimental observations and stress simulation, *Engineering Geology*, 189, 58-67, 2015.
- 1334** Wang, H. F., Bonner, B. P., Carlson, S. R., Kowallis, B. J., and Heard, H. C.: Thermal stress cracking in granite, *Journal of*
1335 *Geophysical Research: Solid Earth*, 94, 1745-1758, <https://doi.org/10.1029/JB094iB02p01745>, 1989.
- 1336** Watkins, H., Bond, C. E., Healy, D., and Butler, R. W. H.: Appraisal of fracture sampling methods and a new workflow
1337 to characterise heterogeneous fracture networks at outcrop, *Journal of Structural Geology*, 72, 67-82,
1338 <https://doi.org/10.1016/j.jsg.2015.02.001>, 2015.
- 1339** Weiserbs, B. I.: The morphology and history of exfoliation on rock domes in the Southeastern United States, *Geography and Earth*
1340 *Sciences*, The University of North Carolina Charlotte, ProQuest, 2017.
- 1341** Weiss, M.: Techniques for estimating fracture size: A comparison of methods, *International Journal of Rock Mechanics and Mining*
1342 *Sciences*, 45, 460-466, <https://doi.org/10.1016/j.ijrmms.2007.07.010>, 2008.
- 1343** Wenk, H.-R.: Some roots of experimental rock deformation, *Bulletin de Mineralogie*, 102, 195-202,
1344 <https://doi.org/10.3406/bulmi.1979.7277>, 1979.
- 1345** West, N., Kirby, E., Bierman, P. R., and Clarke, B. A.: Aspect-dependent variations in regolith creep revealed by meteoric ¹⁰Be,
1346 *Geology*, 42, 507-510, 10.1130/g35357.1, 2014.
- 1347** Wohl, E. E.: The effect of bedrock jointing on the formation of straths in the Cache la Poudre River drainage, Colorado Front
1348 Range, *Journal of Geophysical Research: Earth Surface*, 113, <https://doi.org/10.1029/2007JF000817>, 2008.
- 1349** Wolman, M. G.: A method of sampling coarse river-bed material, *Eos, Transactions American Geophysical Union*, 35, 951-956,
1350 <https://doi.org/10.1029/TR035i006p00951>, 1954.
- 1351** Wu, H. and Pollard, D. D.: An experimental study of the relationship between joint spacing and layer thickness, *Journal of*
1352 *Structural Geology*, 17, 887-905, [https://doi.org/10.1016/0191-8141\(94\)00099-L](https://doi.org/10.1016/0191-8141(94)00099-L), 1995.
- 1353** Zeeb, C., Gomez-Rivas, E., Bons, P. D., and Blum, P.: Evaluation of sampling methods for fracture network characterization using
1354 outcrops, *AAPG Bulletin*, 97, 1545-1566, 10.1306/02131312042, 2013.
- 1355** Zhang, C., Hu, X., Wu, Z., and Li, Q.: Influence of grain size on granite strength and toughness with reliability specified by normal
1356 distribution, *Theoretical and Applied Fracture Mechanics*, 96, 534-544, <https://doi.org/10.1016/j.tafmec.2018.07.001>, 2018.
- 1357** Zhang, L.: Determination and applications of rock quality designation (RQD), *Journal of Rock Mechanics and Geotechnical*
1358 *Engineering*, 8, 389-397, <https://doi.org/10.1016/j.jrmge.2015.11.008>, 2016.
- 1359** Zhou, W., Shi, G., Wang, J., Liu, J., Xu, N., and Liu, P.: The influence of bedding planes on tensile fracture propagation in shale
1360 and tight sandstone, *Rock Mechanics and Rock Engineering*, 55, 1111-1124, 10.1007/s00603-021-02742-2, 2022.
- 1361**

FIGURE 1

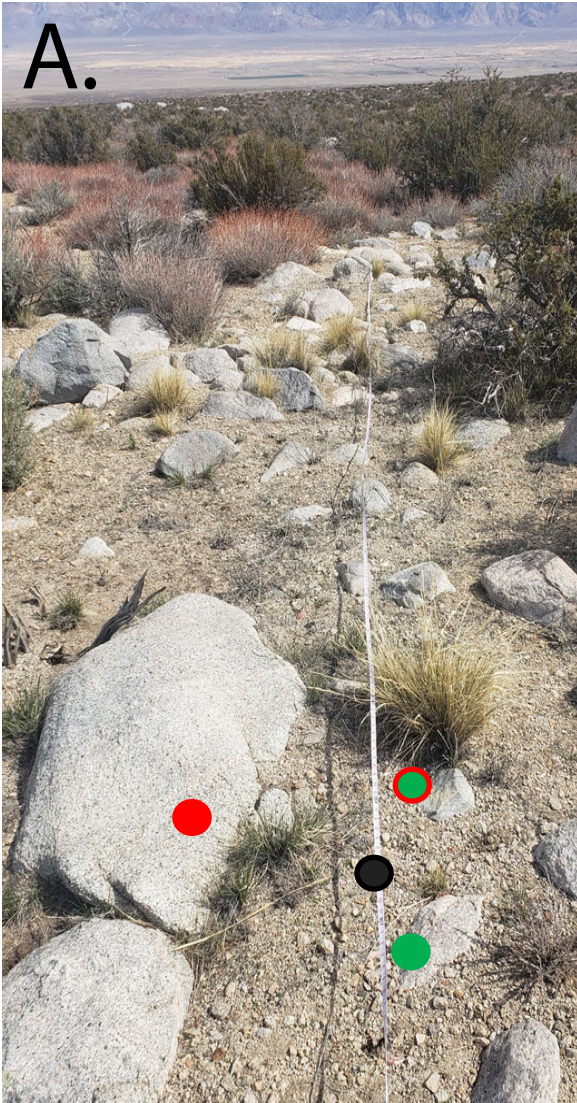


FIGURE 2

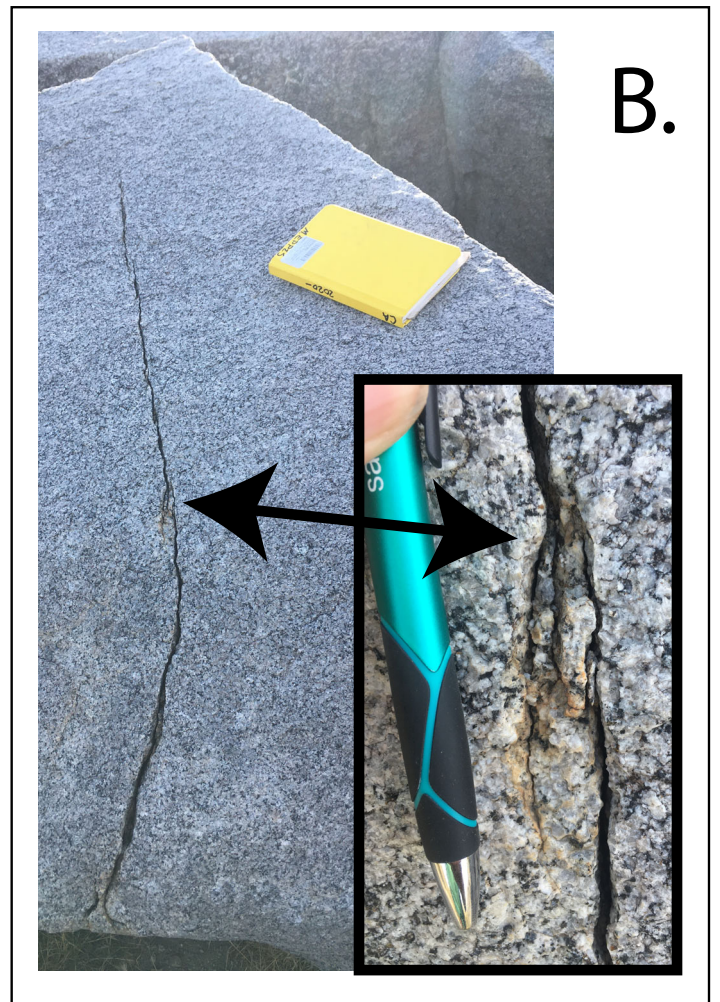


FIGURE 3

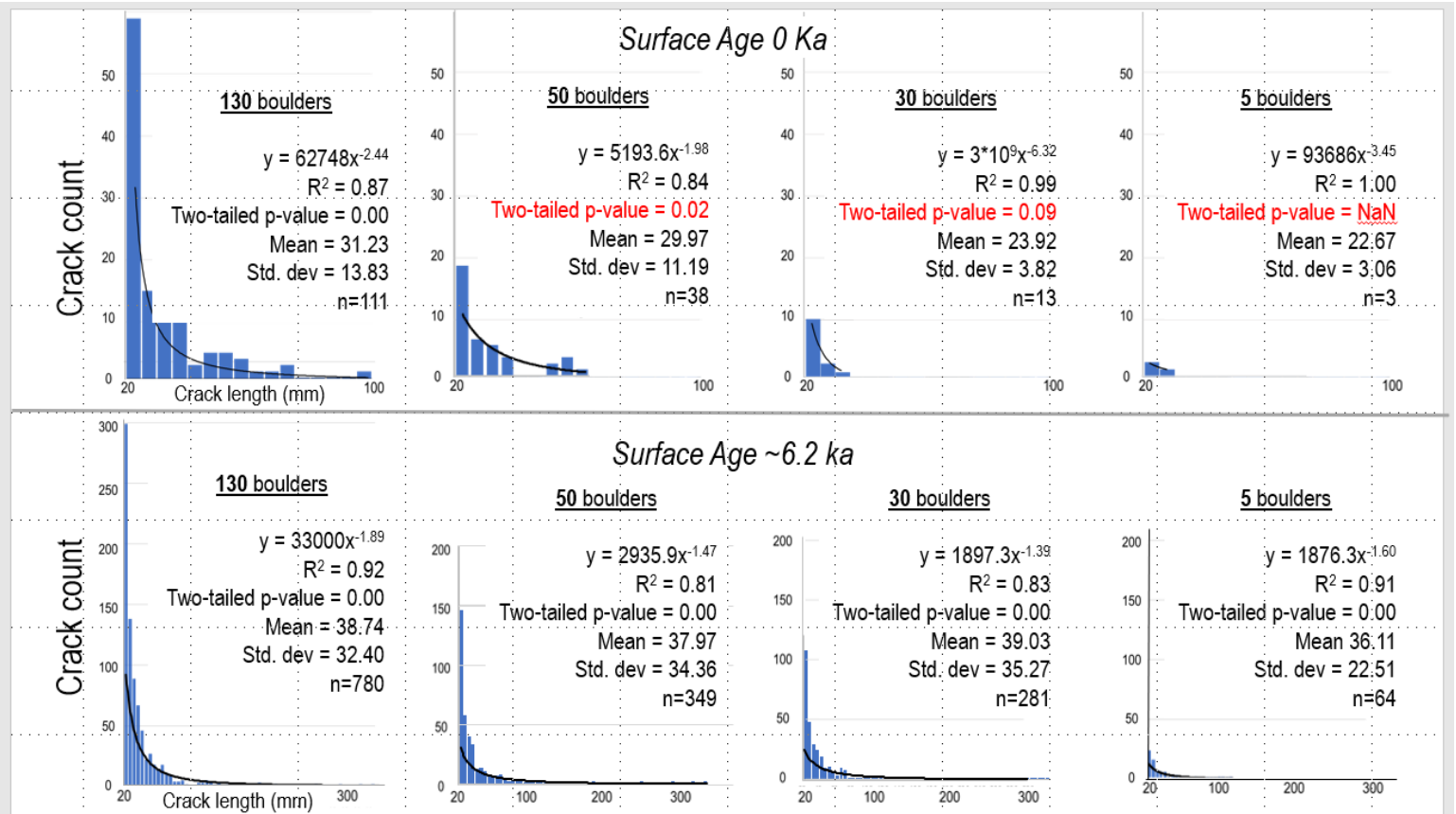


Fig. 3

FIGURE 4

Name(s) & Date: _____ Criteria for Clast/Outcrop selection: _____ Relevant Cl, O, R, P, T observations: _____
 Site Name: _____ Vegetation-type & percent of each: _____
 GPS Coordinates: _____ open ground cover (%): _____
 GPS Projection: _____ Portion observed (eg. All exposed, north face only, etc.): _____ Surface Slope: _____
 Orientation conventions: _____ Other: _____
 Declination: _____

ID & Rock Type	Avg. Grain Size (mm)	spheri- city/ round- ness	Minerology	Length (cm)	Width (cm)	Height (cm)	Exposure	Cracks cm	GD & Pit	Lichen	Varnish	Fabric Type	Fabric Strike (°)	Fabric Dip (°)	Crack ID	Crack Parallel to	Mid Crack Width (mm)	Crack Max Width (mm)	Crack Length (mm)	Crack Strike (°)	Crack Dip (°)	Sheet Ht. (mm)	Weathering Index	Notes	
s- r-							0123	012345	gp	012345	012345	FSBVO				S F L							1 2 3 4 5		
s- r-							0123	012345	gp	012345	012345	FSBVO				S F L								1 2 3 4 5	
s- r-							0123	012345	gp	012345	012345	FSBVO				S F L								1 2 3 4 5	
s- r-							0123	012345	gp	012345	012345	FSBVO				S F L								1 2 3 4 5	
s- r-							0123	012345	gp	012345	012345	FSBVO				S F L								1 2 3 4 5	
s- r-							0123	012345	gp	012345	012345	FSBVO				S F L								1 2 3 4 5	
s- r-							0123	012345	gp	012345	012345	FSBVO				S F L								1 2 3 4 5	
s- r-							0123	012345	gp	012345	012345	FSBVO				S F L								1 2 3 4 5	
s- r-							0123	012345	gp	012345	012345	FSBVO				S F L								1 2 3 4 5	
s- r-							0123	012345	gp	012345	012345	FSBVO				S F L								1 2 3 4 5	
s- r-							0123	012345	gp	012345	012345	FSBVO				S F L								1 2 3 4 5	
s- r-							0123	012345	gp	012345	012345	FSBVO				S F L								1 2 3 4 5	
s- r-							0123	012345	gp	012345	012345	FSBVO				S F L								1 2 3 4 5	
s- r-							0123	012345	gp	012345	012345	FSBVO				S F L								1 2 3 4 5	
s- r-							0123	012345	gp	012345	012345	FSBVO				S F L								1 2 3 4 5	
s- r-							0123	012345	gp	012345	012345	FSBVO				S F L								1 2 3 4 5	
s- r-							0123	012345	gp	012345	012345	FSBVO				S F L								1 2 3 4 5	
s- r-							0123	012345	gp	012345	012345	FSBVO				S F L								1 2 3 4 5	
s- r-							0123	012345	gp	012345	012345	FSBVO				S F L								1 2 3 4 5	
s- r-							0123	012345	gp	012345	012345	FSBVO				S F L								1 2 3 4 5	
s- r-							0123	012345	gp	012345	012345	FSBVO				S F L								1 2 3 4 5	
s- r-							0123	012345	gp	012345	012345	FSBVO				S F L								1 2 3 4 5	
s- r-							0123	012345	gp	012345	012345	FSBVO				S F L								1 2 3 4 5	
s- r-							0123	012345	gp	012345	012345	FSBVO				S F L								1 2 3 4 5	
s- r-							0123	012345	gp	012345	012345	FSBVO				S F L								1 2 3 4 5	
s- r-							0123	012345	gp	012345	012345	FSBVO				S F L								1 2 3 4 5	

Cracks <2 cm: Evidence of microcracks <2 cm long, 0 = 0; 1 = <1/dm²; 2 = 1-5/dm²; 3 = 5-10/dm²; 4 = 10-20/dm²
 GD & Pit: G = positive evidence of granular disintegration (loose grains) P = pitting evident
 Crack length defined as total exposed length of the crack; equivalent to a surface exposure length NOT a 'caliper' length.
 Fabric type: f=foliation; s=fossils; b=bedding; v = vein or dyke o=other
 Lichen & varnish: 0 = 0%, 1 =>0 and <10; 2 =>10 and <30; 3 =>30 and <60; 4 = >60 and <90; 5 =>90
 Avg. Grain Size = representative size of grains throughout the boulder
 Parallel: S = surface, F = fabric, L = long axis of clast or outcrop
 Sheet Ht = the height of the spall or exfoliation resulting from a surface-parallel crack; n/a for other cracks

Crack Parallel to: S: Surface, F: Fabric (joints, bedding); L = long axis
 weathering index:
 0 = no crack (step)
 1: fresh with evidence of recent rupture (flakes/pieces)
 2: sharp, no rounded edges anywhere
 3: mostly sharp with occasional rounded edges
 4: mostly rounded edges with occasional sharp
 5: all rounded edges
 NOTE: 0, or 1 must have clear evidence of a recent break: i.e. small pieces left

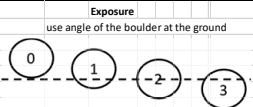


FIGURE 5

Feature (crack, fossil, pore)
Size Classes (mm)

VC = Very Coarse (>20)
C = Coarse (<10 and >5)
M = Medium (<5 and >2)
F = Fine (<2 and >1)
VF = Very Fine (<1)

Quantity Classes

'1' - Few: < 1 per area
 '2' - Common: 1-5 per area
 '3' - Very common: > 5 and < 10 per area
 '4' - Many: ≥ 10 per area

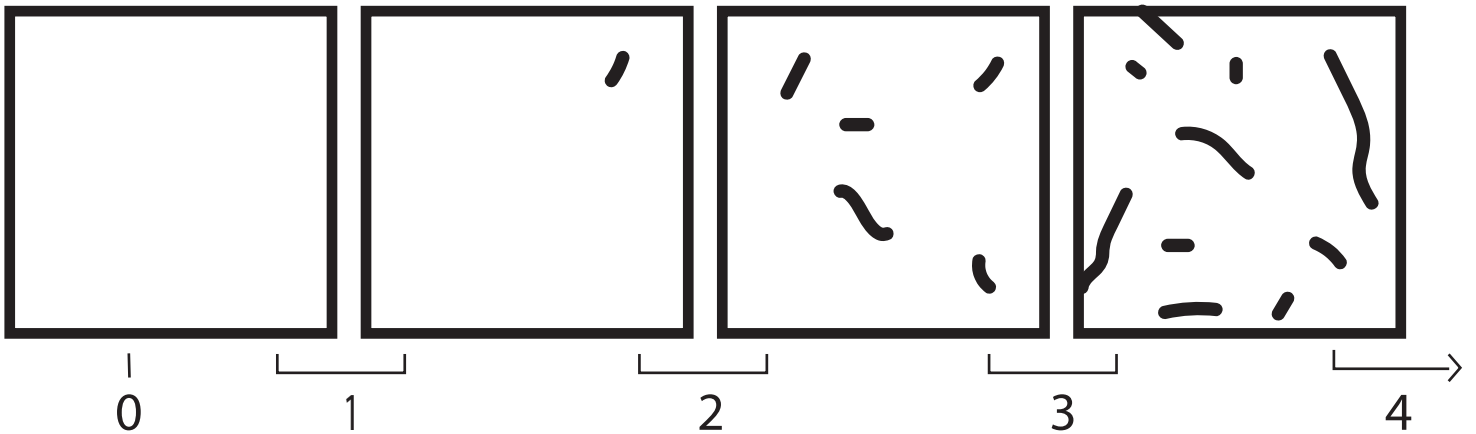
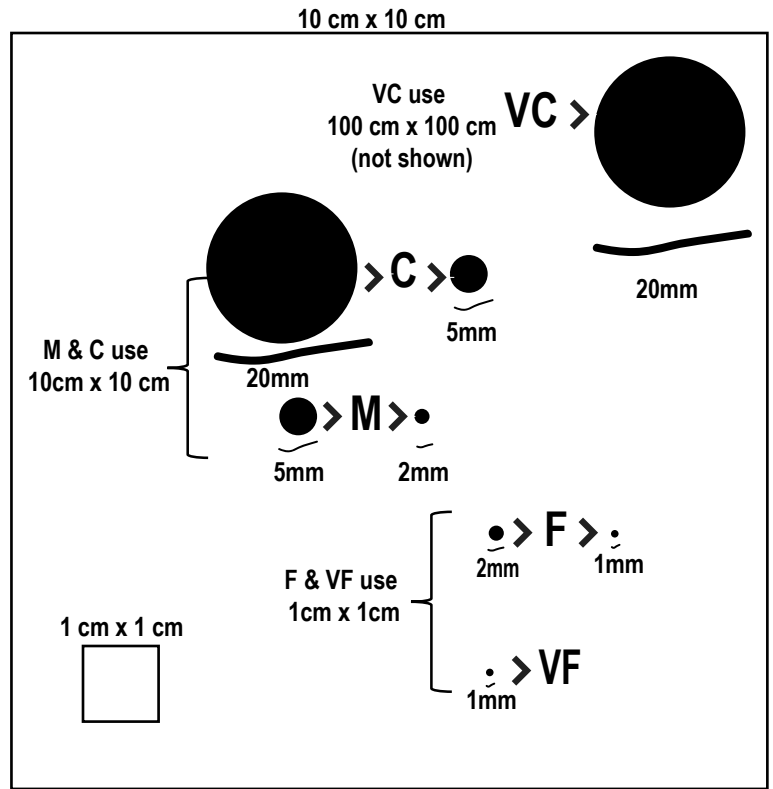


FIGURE 6

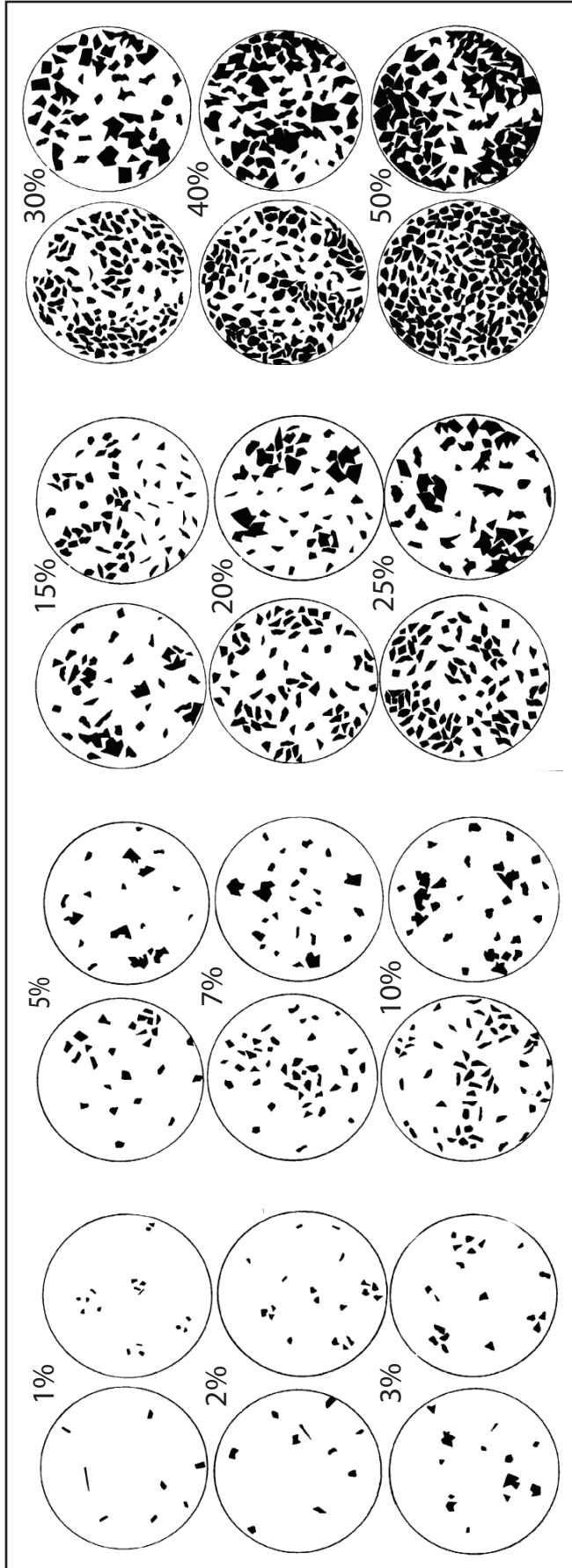
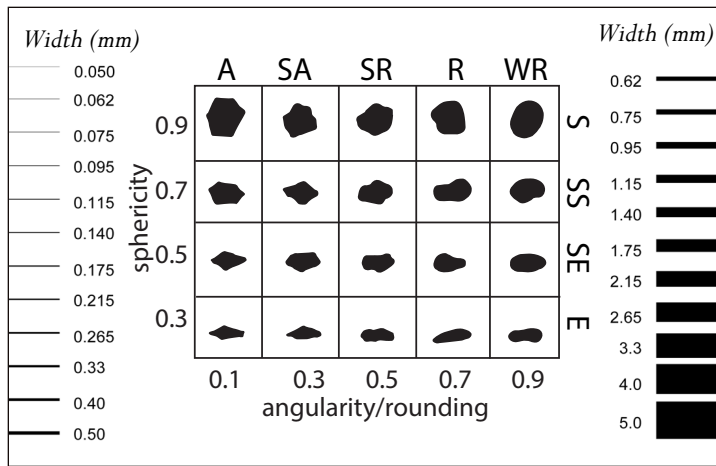


FIGURE 7



note to copy-editor: this figure should be published to scale when the document is viewed at 100%

FIGURE 8

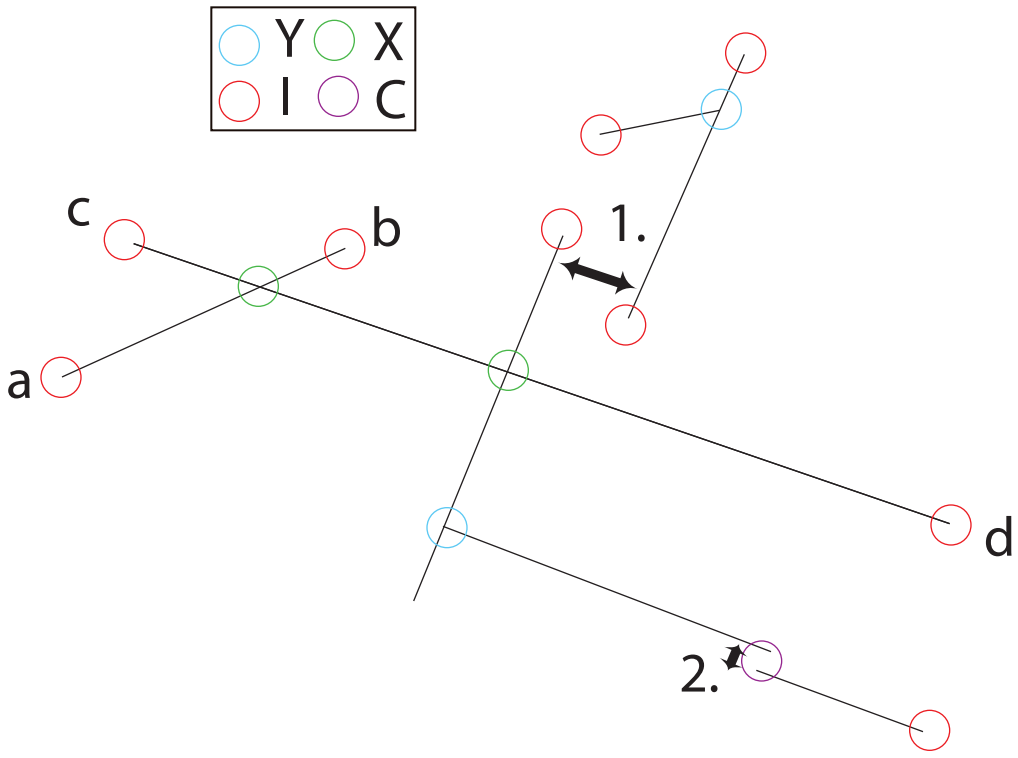


FIGURE 9

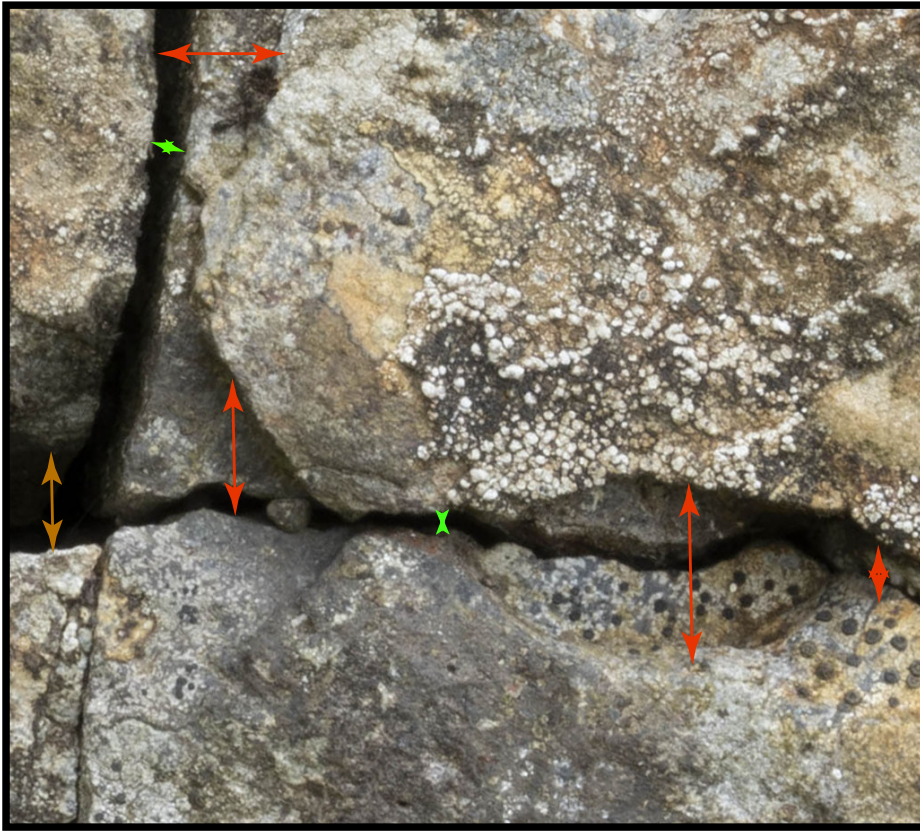


FIGURE 10

